The Laser*

A. YARIV†, MEMBER, IRE, AND J. P. GORDON†

Summary—**This article is intended as a review of the field of optical masers, or lasers as they have come to be known, summarizing both theory and practice. It starts with a theoretical section in which black body radiation theory is used to introduce the concepts of spontaneous and induced transitions. This is followed by the derivation of the Schawlow-Townes instability (start-oscillation) condition and a description of the different laser media. Other topics treated include: optical pumping, experimental techniques, output power and noise. The sections on optical resonators and communications which conclude the paper have been slightly emphasized since, perhaps to a larger extent than the other topics covered in this paper, they coincide with traditional areas of interest of microwave and communications engineers.**

I. Introduction

THE FEASIBILITY of maser action at optical and near optical frequencies was considered in a paper by Schawlow and Townes[1] in 1958. In 1960, less than two years later, Maiman[2] succeeded in operating a pulsed ruby laser. The first continuous wave (CW) laser was Javan's[3] He-Ne gas laser announced in January, 1961. This was followed a year later by the attainment of CW laser action in three solid systems.[4–6]

The first two years following the demonstration of Maiman's ruby laser were characterized by an intense and fruitful search for new laser media. More recently, as an ever increasing number of workers have joined the field, the investigations have been extended to include studies of laser characteristics and applications.

This paper is intended as a review of the laser field as it stands today.

II. Black Body Radiation Theory

Since a number of fundamental concepts which are used in laser theory can be introduced through the use of black body radiation theory we shall rederive, in this section, some of the more important results of this theory.

Assume a cubic box with dimensions L whose side walls are kept at temperature T. Let the radiation field inside this enclosure be described by the vector potential $\boldsymbol{A}$. A typical Cartesian component of $\boldsymbol{A}$, say A_x, satisfies

$$\nabla^2 A_x(r, t) - \frac{1}{c^2}\frac{\partial^2 A_x(r,t)}{\partial t^2} = 0. \tag{1}$$

If we require that the field be periodic in L we can, by Fourier's theorem, expand a typical field component, say A_x, as

$$A_x(r, t) = \sum_{l,m,n=-\infty}^{+\infty} A_{l,m,n}^{(x)}(t) \exp\left[i\boldsymbol{k}\cdot\boldsymbol{r}\right] \tag{2}$$

where the wave vector $\boldsymbol{k}$ is given by

$$k_x = \frac{2\pi l}{L}$$

$$k_y = \frac{2\pi m}{L}$$

$$k_z = \frac{2\pi n}{L}. \tag{3}$$

If we substitute (2) into (1) and assume a time dependence $e^{i\omega t}$ for the l, m, n, field component we get

$$\frac{\omega^2}{c^2} = k^2 = (k_x^2 + k_y^2 + k_z^2). \tag{4}$$

From (3) it follows that with each mode we can associate a volume of $dk_x dk_y dk_z = (2\pi/L)^3$ in $\boldsymbol{k}$ space. The number of modes N_k whose wave vectors have magnitudes between 0 and k is derived simply by dividing the total volume in $\boldsymbol{k}$ space $4/3\,\pi k^3$ by the volume per mode $(2\pi/L)^3$ and by multiplying the result by two, since for each wave vector $\boldsymbol{k}$ there are two possible directions of polarization. The result is

$$N_k = \frac{k^3 L^3}{3\pi^2},$$

or, using $k = 2\pi\nu/c$,

$$\frac{N_\nu}{V} = \frac{8\pi\nu^3}{3c^3} \tag{5}$$

for the total number of modes per unit volume between $\nu = 0$ and ν. The mode density per unit frequency $p(\nu)$ is given by

$$p(\nu) = \frac{1}{V}\frac{dN(\nu)}{d\nu} = \frac{8\pi\nu^2}{c^3}. \tag{6}$$

* Received November 8, 1962.

† Bell Telephone Laboratories, Inc., Murray Hill, N. J.

[1] A. L. Schawlow and C. H. Townes, "Infrared and optical masers," *Phys. Rev.*, vol. 112, pp. 1940–1949; December, 1958.

[2] T. H. Maiman, "Stimulated optical radiation in ruby masers," *Nature*, vol. 187, pp. 493–494; August, 1960.

[3] A. Javan, W. B. Bennett, Jr., and D. R. Herriott, "Population inversion and continuous optical maser oscillation in a gas discharge containing a He-Ne mixture," *Phys. Rev. Lett.*, vol. 6, pp. 106–110; February 1961.

[4] L. F. Johnson, G. D. Boyd, K. Nassau, and R. R. Soden, "Continuous operation of the $CaWO_4:Nd^{3+}$ optical maser," PROC. IRE (*Correspondence*), vol. 50, p. 213; February, 1962.

[5] D. F. Nelson and W. S. Boyle, "A continuously operating ruby optical maser," *Appl. Optics*, vol. 1, pp. 181–183; March, 1962.

[6] G. D. Boyd, R. J. Collins, S. P. S. Porto, A. Yariv, and W. A. Hargreves, "Excitation, relaxation, and continuous maser action in the 2.613 micron transition of $CaF_2:U^{3+}$ masers," *Phys. Rev. Lett.*, vol. 8, pp. 269–272; April, 1962.

The black body radiation density per unit frequency interval (joule/m³-cps) $\rho(\nu)$ is equal to the product of $p(\nu)$ and the average energy per mode $\overline{E}$, which is derived from Planck's hypothesis

$$\overline{E} = \frac{\sum_{n=0}^{\infty} nh\nu e^{-nh\nu/kT}}{\sum_{n=0}^{\infty} e^{-nh\nu/kT}} = \frac{h\nu}{e^{h\nu/kT} - 1}, \tag{7}$$

so that

$$\rho(\nu) = \frac{8\pi h\nu^3}{c^3} \frac{1}{e^{h\nu/kT} - 1}. \tag{8}$$

One often characterizes the energy density of a radiation field by specifying the average number of quanta (photons) per mode. This quantity, which we shall call $\bar{n}$, is thus

$$\bar{n} = \frac{\overline{E}}{h\nu} = \frac{1}{e^{h\nu/kT} - 1}. \tag{9}$$

$\bar{n}$ is also referred to, at times, as the excitation number of the radiation field.

III. Spontaneous and Induced Transitions

The concepts of spontaneous and induced transitions are fundamental in laser theory and, although their derivation is based on quantum mechanical concepts, their existence can be demonstrated, qualitatively, with the aid of classical electrodynamics.

Spontaneous Transitions

In the classical theory when an electron oscillates with frequency ν in a harmonic potential well so that its distance from the equilibrium position is given by

$$r = r_0 e^{i2\pi\nu t}, \tag{10}$$

it would radiate energy at a rate P_R given by

$$P_R = \frac{16\pi^4 m_0^2 \nu^4}{3c^3} \tag{11}$$

where c is the velocity of light in the medium and $m_0 = er_0$ is the amplitude of the electric dipole moment. Since the total energy (twice the average kinetic energy) is

$$E = \frac{2m\pi^2\nu^2 m_0^2}{e^2} \tag{12}$$

the spontaneous decay time constant of the energy is given by $\tau_{\text{class}} = E/P_R$

$$\tau_{\text{class}} = \frac{3mc^3}{8\pi^2\nu^2 e^2} \tag{13}$$

which is referred to as the classical lifetime of the electron.

In quantum mechanics we are concerned with an atom[7] which at some time, say $t=0$, is known to be in level 2 (see Fig. 1). The atom has a finite probability per unit time of undergoing a transition to level 1 with the consequent emission of a photon of energy $h\nu_{12}$. This transition rate A, being independent of any forcing radiation field, is referred to as the spontaneous transition rate. With each of the two levels is associated a wave function, ψ_2 for level 2 and ψ_1 for level 1, whose significance is such that $|\psi_1(r)|^2 dV$, for example, is the probability of finding the electron (assuming for simplicity that we are dealing with an atom having a single unpaired electron) in the volume dV, assuming that in fact the atom is in state 1 thus

$$\int_{\text{whole space}} |\psi_1(r)|^2 dV = \int_{\text{whole space}} |\psi_2(r)|^2 dV = 1.$$

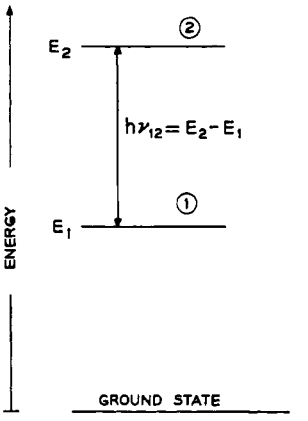

Fig. 1—A three-level energy system.

We can now associate with each state a dipole moment whose definition is analogous to the dipole moment of a classical charge distribution $\rho(r) = e|\psi(r)|^2$

$$M_{11} = e\int r\psi_1\psi_1^* dV = er_{11}$$

$$M_{22} = e\int r\psi_2\psi_2^* dV = er_{22}$$

but, and here one departs from classical theory, there is a separate dipole moment M_{12} associated with the transition $1 \leftrightarrow 2$

$$M_{12} = e\int r\psi_1^*\psi_2 dV = er_{12} \tag{14}$$

and it is this dipole moment which oscillates a frequency ν_{12} which plays a role similar to its classical counterpart $m_0 e^{i\omega t}$ in limiting the lifetime of the atom in the excited level 2. The spontaneous emission life-

[7] L. I. Schiff, "Quantum Mechanics," McGraw-Hill Book Co., Inc., New York, N. Y., 2nd. ed., p. 261; 1955.

time for a 2→1 dipole transition can be shown from quantum theory[7] to be

$$t_{\text{spont}} = \frac{1}{A} = \frac{3hc^3}{8\pi e^2\omega^3 r_{21}^2} \tag{15}$$

where the spontaneous transition rate A is defined by (15).

Induced Transitions

If the oscillating electron, treated at the beginning of this section, is subjected to an external electric field

$$\epsilon = \epsilon_0 e^{i\omega t}$$

it is a simple matter to show that its total energy will decay with an initial "time constant"

$$\tau = \frac{m\omega r_0}{e\epsilon_0 \cos\phi}, \tag{16}$$

where ϕ is the phase difference between the electron's velocity and the field ϵ. The electron can either lose energy to the driving field or gain energy from it, depending on the sign of $\cos\phi$. This process, because of its dependence on the external driving field, can be characterized as an induced process. The main difference between the spontaneous and induced processes is the dependence of the induced rate on the field strength and the possibility of power flow in both directions in the induced case. The quantum mechanical analysis, which follows, shows that under the influence of an external field at frequency ν_{12} the atom can either lose energy by undergoing a 2→1 transition or gain energy by a 1→2 transition. The derivation presented below is similar to the one used originally by Einstein.[8]

If the atomic system is at thermal equilibrium at a temperature T then the populations of level 2 and 1 obey the Boltzmann relation

$$\frac{N_2}{N_1} = e^{-h\nu_{21}/kT}. \tag{17}$$

This is a dynamic equilibrium where in addition to spontaneous 2→1 transitions the atoms undergo both upward and downward induced transitions under the influence of the thermal radiation field. If it is assumed that the induced transition rate is proportional to the black body energy density per unit frequency interval $\rho(\nu)$, the dynamic equilibrium can be expressed as

$$\rho(\nu)B_{12}N_1 = AN_2 + \rho(\nu)B_{21}N_2 \tag{18}$$

which states that the total rate of 1→2 transitions (induced only) is equal to the total rate of 2→1 transitions (both spontaneous and induced). Using (17) in (18) leads to

$$\rho(\nu) = \frac{A}{B_{12}e^{h\nu_{12}/kT} - B_{21}}.$$

For $\rho(\nu)$ to agree with (8) we must have

$$B_{12} = B_{21} = B$$

and

$$\frac{A}{B} = \frac{8\pi h\nu^3}{c^3}.$$

Since the induced transition rate W_i' as defined by (18) is equal to $\rho(\nu)B_{12}$, we get

$$\frac{W_i'}{A} = \rho(\nu)\frac{c^3}{8\pi h\nu^3} \tag{19}$$

or, substituting the value of A from (15),

$$W_i' = \left(\frac{2\pi}{3}\right)\frac{e^2 r_{21}^2}{\hbar^2}\rho(\nu). \tag{20}$$

The usefulness of (19) [or (20)] is limited by the fact that implied in its derivation is the assumption that $\rho(\nu)$ is a constant over the frequency range in which the atomic system can interact with the radiation field, *i.e.*, the frequency range in which the atoms can emit or absorb energy. In laser theory we are chiefly interested in the response of the atomic system to signals of high spectral purity whose energy is distributed over a band of frequencies which is small in comparison to the atomic absorption bandwidth. Before we can obtain an expression for the transition rate for this case it is necessary to introduce the concept of the atomic line shape function $g(\nu)$. There are a number of equivalent ways of defining $g(\nu)$. We will use the definition that $g(\nu)d\nu$ is the probability that a given transition will result in an emission (or absorption) of a photon with energy between $h\nu$ and $h(\nu+d\nu)$. It follows that

$$\int_0^\infty g(\nu)d\nu = 1 \tag{21}$$

and that a plot of $g(\nu)$ vs ν is identical with the normalized absorption (or emission) plot in which the absorption (or emission) intensity is plotted against ν. The origin of this distribution may be due to a spread in the Doppler shifts as in the case of low-pressure gas atoms, or to an actual spread in the position of the energy levels. The first mechanism is usually responsible for $g(\nu)$ in gas lasers while the second is believed to predominate in the case of solid-state lasers. The term inhomogeneous, or static, broadening is often used to describe both these two cases. The term homogeneous broadening is reserved for cases where the finite line-

[8] A. Einstein, "Zur Quanten Theorie der Strahlung," *Phys. Zeit.*, vol. 18, pp. 121–128; March, 1917.

width results from a limited coherence time for the individual atoms[9] as in the case of relaxation.

If we rewrite (19) in the form

$$\frac{W_i'g(\nu)d\nu}{Ag(\nu)d\nu} = \frac{\rho(\nu)c^3}{8\pi h\nu^3}, \tag{22}$$

it is clear from the definition of $g(\nu)d\nu$ that $Ag(\nu)d\nu$ is the spontaneous transition rate into $d\nu$, *i.e.*, resulting in an emission of a photon of frequency between ν and $\nu+d\nu$, while $W_i'g(\nu)d\nu$, which according to (22) can be written as

$$W_i'g(\nu)d\nu = \rho(\nu)d\nu Ag(\nu)\frac{c^3}{8\pi h\nu^3}, \tag{22a}$$

is the induced transition rate into $d\nu$ due to radiation of density $\rho(\nu)$ per unit frequency interval. Now $I(\nu)d\nu = c\rho(\nu)d\nu$ is the energy flux (watts/m^2) due to frequencies between ν and $\nu+d\nu$ so that (22a) can be rewritten as

$$W_i'g(\nu)d\nu = \frac{c^2}{8\pi h\nu^3 t_{\text{spont}}}g(\nu)I(\nu)d\nu. \tag{23}$$

If the transitions are induced by a monochromatic signal whose energy flux is I_ν watts/m^2 we have

$$I(\nu) = I_\nu\delta(\nu' - \nu)$$

where $\delta(\nu-\nu')$ is the Dirac delta function. Substituting this into (23) and integrating both sides over all frequencies leads to an expression for the total transition rate $W_i(\nu)$ due to the monochromatic signal

$$\boxed{W_i(\nu) = \frac{c^2}{8\pi h\nu^3 t_{\text{spont}}}g(\nu)I_\nu} \tag{24}$$

which is the form we will find most useful.[10]

Let us return to (19). From (8) and (9) we can see that $\rho(\nu)$ is given by

$$\rho(\nu) = \frac{8\pi h\nu^3}{c^3}\bar{n}$$

which when substituted into (19) gives

$$\frac{W_i'}{A} = \bar{n}. \tag{25}$$

W_i' and A apply to transitions into the whole linewidth, but since the dynamic thermal equilibrium considerations used in deriving (19) must apply to any portion of the line, for instance the portion of the line that corresponds to a single resonator mode, we can also write

$$\frac{(W_i)\text{ mode}}{(W_{\text{spont}})\text{ mode}} = \bar{n}, \tag{26}$$

which when stated in words reads "The ratio of the induced transition rate to the rate of spontaneous emission into a given mode is equal to the number of quanta, $\bar{n}$, in the mode." Eq. (26) is a more specialized form of (24) which proves useful in certain applications. As a matter of fact it is the form used originally by Schawlow and Townes[1] to derive the laser oscillation condition.

IV. The Start Oscillation Condition

A laser consists of an amplifying atomic medium occupying all or part of the volume of a suitable resonator. The role of the resonator is to maintain an electromagnetic field configuration (ideally one corresponding to a single resonant mode) whose losses are replenished by the amplifying medium through induced emission. We shall derive the instability (start-oscillation) condition by requiring that the induced power be equal to that lost by the resonator. The optical resonators used in lasers consist usually of a cylindrical region (solid crystal or gas envelope) with two opposing plane parallel or curved reflectors at right angles to the cylindrical axis. The oscillation consists essentially of a standing wave generated by a plane wave bouncing back and forth between the two reflectors. A number of loss mechanisms are operative in attenuating the wave. The most important ones are:

1) Transmission and absorption in the mirrors.
2) Absorption in the amplifying medium due to mechanisms other than 1-2 transitions.
3) Scattering by optical inhomogeneities.[11]
4) Diffraction by the mirror apertures.
5) Mode conversion; this actually includes loss mechanism 3), but is more general. This accounts, for instance, for losses due to imperfect mirrors.

For the purpose of this section it is sufficient to characterize all the loss mechanisms by a single parameter t_{photon}, which is equal to the decay time constant of the radiation in a given mode presuming the amplifying medium is rendered neutral, *i.e.*, $N_1 = N_2$. t_{photon} is related to the total loss per pass α (for simplicity we assume the two mirrors to be identical) and to the con-

[9] A. M. Portis, "Inhomogeneous line broadening in F-centers," *Phys. Rev.*, vol. 91, pp. 1071–1078; September, 1953.

[10] Expressing W_i in terms of t_{spont} is valid only for isotropic and cubic media. If the symmetry is lower than cubic, W_i will depend on the direction of polarization of the inducing radiation. Eq. (24) can still be used provided we replace t_{spont} in (24) by (15).

[11] W. Kaiser and M. J. Keck, "Scattering losses in optical maser crystals," *J. Appl. Phys.*, vol. 33, pp. 762–764; February, 1962.

ventionally used quality factor Q by

$$t_{\text{photon}} = \frac{L}{\alpha c} = \frac{Q}{2\pi\nu}, \tag{27}$$

where c is the velocity of light in the medium (the same definition applies throughout this paper) and L is the distance between mirrors. Eq. (27) is valid only for $\alpha \ll 1$.

The increase in mode intensity I due to induced emission is given by

$$\left(\frac{dI}{dt}\right)_1 = h\nu\left(n_2 - n_1\frac{g_2}{g_1}\right)cW_i$$

where the factor g_2/g_1 is introduced to take care of cases where the degeneracy[12] g_2 of level 2 and that of level 1 (g_1) are not equal. n_2 and n_1 are the population densities of levels 2 and 1, respectively. The loss of intensity is described by

$$\left(\frac{dI}{dt}\right)_2 = -\frac{I}{t_{\text{photon}}}.$$

For sustained oscillation the condition

$$\left(\frac{dI}{dt}\right)_1 + \left(\frac{dI}{dt}\right)_2 \gtrless 0$$

must be fulfilled, which enables us, upon substitution of W_i from (24), to obtain the condition

$$\boxed{\left(n_2 - n_1\frac{g_2}{g_1}\right) = \frac{8\pi t_{\text{spont}}\nu^2}{c^3 g(\nu_c) t_{\text{photon}}} = \Delta N_c/V \quad \text{at threshold}} \tag{28}$$

for oscillation near the line center ν_c. This is our main result for this section.

ΔN_c is defined by (28) and is referred to throughout this paper as the critical (at threshold) population inversion. $\Delta N_c/V$ is the critical inversion density. It is to be noted that $\Delta N_c/V$ depends only on a single resonator parameter $-t_{\text{photon}}$.

If $g(\nu)$ has a Lorentzian shape with full width at half-maximum of $\Delta\nu$ centered about ν_c, then

$$g(\nu) = \frac{\Delta\nu}{2\pi\left[(\nu - \nu_c)^2 + \left(\frac{\Delta\nu}{2}\right)^2\right]} \tag{29}$$

[12] It is possible for a number of atomic states to possess the same energy level, in which case we refer to the level as being g-fold degenerate where g is the number of states.

and $g(\nu_c) = 2/\pi\Delta\nu$ so that the oscillation condition becomes

$$n_2 - n_1\frac{g_2}{g_1} \gtrless \frac{4\pi^2\nu^2\Delta\nu}{c^3}\left(\frac{t_{\text{spont}}}{t_{\text{photon}}}\right) \tag{30}$$

for a Gaussian $g(\nu)$, $g(\nu_c) = 2(\pi \ln 2)^{1/2}/\pi\Delta\nu$ and the start-oscillation condition is still given by (30) with $\Delta\nu$ replaced by $\Delta\nu/(\pi \ln 2)^{1/2}$.

It is sometimes desirable to have an expression relating the power gain per unit length γ to the inverted population density. The gain parameter γ is given by

$$\gamma = \frac{dI(\nu)}{dz} \Big/ I(\nu) = \frac{\left(n_2 - n_1\frac{g_2}{g_1}\right)h\nu}{I(\nu)} W_i,$$

which by (24) becomes

$$\gamma = \frac{(\pi \ln 2)^{1/2}c^2\left(n_2 - n_1\frac{g_2}{g_1}\right)}{4\pi^2\nu^2 t_{\text{spont}}\Delta\nu} \tag{31}$$

where we used $g(\nu_c) = 2(\pi \ln 2)^{1/2}/\pi\Delta\nu$, which is appropriate for a Gaussian line with full width at half-maximum equal to $\Delta\nu$.

The strength of optical transitions is often characterized by an "oscillator strength" f which is defined as[13]

$$f = \frac{mc}{\pi\left(n_1\frac{g_2}{g_1} - n_2\right)e^2}\int_0^\infty \alpha(\nu)d\nu, \tag{32}$$

where the radiation density at ν decays as $e^{-\alpha z}$. It can be shown[13] that (32) is consistent with the relations

$$f = \frac{1}{3}\frac{\tau_{\text{classical}}}{t_{\text{spont}}} = \frac{mc^3}{2e^2\omega^2 t_{\text{spont}}}. \tag{33}$$

Using (33) we can rewrite (31) as

$$\gamma = \frac{2(\pi \ln 2)^{1/2}\left(n_2 - n_1\frac{g_2}{g_1}\right)e^2 f}{mc\Delta\nu}; \tag{34}$$

and since the start-oscillation condition is $\gamma = l$, where l is the total loss per pass (in nepers) divided by the resonator's length, we can also write

$$n_2 - n_1\frac{g_2}{g_1} = \frac{mc\Delta\nu l}{2(\pi \ln 2)^{1/2}e^2 f} \tag{35}$$

[13] See, for instance, R. W. Ditchburn, "Light," Interscience Publishers, Inc., New York, N. Y., 1st ed., pp. 455, 460, and 576.

for the start-oscillation condition. This form is quite useful because many tabulations (see for instance Corliss & Bozman[14]) give f for a great variety of observed transitions.

Another useful form of the oscillation condition, the one originally given by Schawlow and Townes,[1] results when we multiply both sides of (30) by V (the mode volume), recognize $8\pi\nu^2/c^3$ as $p(\nu)$, and define

$$p = \frac{\pi V}{2} p(\nu)\Delta\nu. \tag{36}$$

The number p may be thought of as the number of modes "on speaking terms" with the atomic transition. The result of these substitutions is

$$\Delta N_c = p \frac{t_{\text{spont}}}{t_{\text{photon}}}, \tag{37}$$

where it should be noted that t_{spont} may not be equal to the observed lifetime t_2. Its basic definition is that of (15).

V. Minimum Pumping Power for Four- and Three-Level Lasers

The discussion up to this point was based on a hypothetical $2\leftrightarrow 1$ transition and was not concerned with how the levels 2 and 1 fit into the energy levels scheme of the atom. This detached point of view must be abandoned when one tries to find answers to some mundane questions, as "How much power does it take to maintain laser oscillation in a given material?" and others of similar practical nature. Before launching on a detailed description of different laser media it proves useful to divide them into two broad categories illustrated in Fig. 2.

The four-level laser is characterized by having a terminal level 1 whose thermal equilibrium population N_1 is small compared to the critical inversion ΔN_c. The oscillation condition for this laser becomes

$$N_2 \approx \Delta N_c. \tag{38}$$

For level 1 to be sufficiently depopulated its separation from the ground state E_1 must be considerably larger than kT. For most of the solid-state lasers the condition $E_1 \gtrsim 8kT$ is sufficient.

On the threshold of oscillation we must maintain $N_2 \approx \Delta N_c$ atoms in level 2. This involves a minimum expenditure of power

$$P_{fc} = \frac{\Delta N_c h\nu}{t_{\text{spont}}} = \frac{ph\nu}{t_{\text{photon}}}. \tag{39}$$

The subscript f stands for fluorescence and c for the word critical, since P_{fc} is exactly the fluorescence power at threshold. We have made use of (37) and (38). Using (36) we get

$$P_{fc} = \frac{4\pi^2 h\nu^3 V\Delta\nu}{c^3 t_{\text{photon}}}. \tag{40}$$

Some numerical estimates of P_{fc} will be given in Section VII.

The second category is that of three-level masers. The terminal level separation from the ground state is smaller than or comparable to kT so that due to thermalization $N_1 \gg \Delta N_c$ and laser action ensues with $N_2 \approx N_1$. It is clear that the minimum pumping power for a four-level laser is smaller than that of a three-level one, all other factors assumed equal, by a factor $\epsilon = \Delta N_c/N_2$, where N_2 is of the order of magnitude of half the total number of active atoms in the crystal. For some typical solid-state crystals $\Delta N_c \sim 10^{16}$ and $N_2 \sim 10^{18}$ so that the increase in pump power in the three-level operation compared to the four-level case is ~ 100. A consideration of degeneracies would not change the substance of the above conclusions and has therefore been avoided.

We can now apply the results of Section V to draw up a list of requirements for laser media. This will be followed by a survey of the materials which have been used, to date, in laser applications.

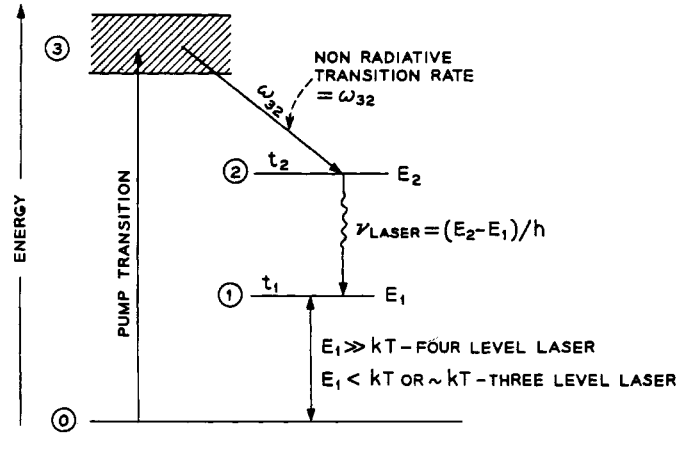

Fig. 2—Three-level and four-level lasers.

VI. Laser Media

Some of the main requirements for laser media are:

1) The atomic linewidth $\Delta\nu$ should be as small as possible [see (40)].
2) The laser medium should have as little absorption as possible at ν_{12} which is due to factors other than the $2\rightarrow 1$ transition. Such absorption is equivalent to shortening the photon lifetime t_{photon}. The excited atoms must not be able to absorb energy at frequency ν_{12}. Such absorption will cause a reduc-

[14] C. H. Corliss and W. R. Bozman, "Experimental Transition Probabilities for Spectral Lines of Seventy Elements," NBS Monograph #53, 1961.

tion in t_{photon} and, in addition, decrease the population of level 2.[15]

3) The terminal level 1 should, preferably, be far enough above the ground state so that $N_1 < \Delta N_c$ and four-level operation will obtain.

4) The lifetime t_2 of the metastable state should, as nearly as possible, be radiative, *i.e.*, $t_2 \sim t_{spont}$.

5) The lifetime t_1 of the terminal level must be smaller than t_2. If $t_1 \geq t_2$, no population inversion can be attained regardless of the pumping strength (see Section IX).

The next two requirements are applicable in the case of optically pumped solid-state lasers.

6) The material should possess broad absorption bands with appreciable absorption strength and high quantum efficiency.[16]

7) The material should be of sufficiently high optical quality so that scattering by optical inhomogeneities[11] does not shorten the photon lifetime appreciably.

Labeling of Energy Levels

There is no single method for denoting energy levels in atoms. The levels of the 4f (rare earth) series ions and the 5f (actinide) series ions are usually designated according to their free ion counterparts.[17] The position of the energy levels in the iron (3d) transition group is so strongly dependent on the crystalline electric field that the free ion designation is abandoned in favor of that of the irreducible representation of the point symmetry group associated with the level.[17]

In the case of the noble gases one often encounters the now obsolete empirical Paschen notation[18] and the modified Racah notation.[18] All of these notations will be used in the description of the different laser media which follows.

4f (Rare Earth) Ions in Crystals

The observed transitions up through the optical range involve the unpaired electrons of the 4f shell ($n=4$, $l=3$). These electrons are well shielded from the crystalline electric field by two 5s and six 5p electrons so that the perturbation of the crystal field on the ion is small and the positions of the energy levels for a given ion are found to be substantially independent of the host crystal into which it is incorporated. The transitions between levels belonging to the 4f configuration are usually narrow and are very often radiative[17,19] and it is therefore no accident that most of the solid-state lasers, listed in Table I (page 13), use rare earth ions. The divalent rare earth ions possess relatively strong absorption bands ($f \sim 10^{-4}$–10^{-3}) in the visible which are due to 4f→5d transitions,[17] as well as sharp fluorescence lines characteristic of the trivalent rare earth ions, which are due to 4f→4f transitions. The 4f→5d transitions in the trivalent ions occur at ultraviolet frequencies and are far less suitable for optical pumping. A listing of all the rare earth ions in which laser action has been obtained is included in Table I. We shall limit the discussion in this section to Nd^{3+} in $CaWO_4$ and Dy^{2+} in CaF_2 which are the only two CW solid-state lasers using rare earth ions.

Our understanding of the energy levels of Nd^{3+} is due mostly to Carlson and Dieke[20] who investigated its visible absorption and fluorescence in $LaCl_3$. Fig. 3 (page 14) includes an energy level diagram taken from Carlson and Dieke.[20]

Johnson and Nassau[21] observed fluorescence radiation at 1.065 μ from Nd^{3+} included substitutionally for Ca^{2+} in a $CaWO_4$ crystal lattice and also obtained laser action at this wavelength. The infrared fluorescence of Nd^{3+} in the crystal originates from the $^4F_{3/2}$ level, and terminates in the various levels of the ground ^4I multiplet. The strongest component of the fluorescence is in the $^4F_{3/2} \rightarrow {}^4I_{11/2}$ group, at 1.065 μ. This transition occurs about 2000 cm^{-1} lower in energy than the highest frequency component of the $^4F_{3/2} \rightarrow {}^4I_{9/2}$ fluorescence. Hence the terminal level is about 2000 cm^{-1} above the "ground" state, and so laser action should occur with no marked rise in threshold at least up to room temperature. This is as observed. The strongest fluorescence component has a width $\Delta\nu$ of about 7 cm^{-1} at 77°K, and includes about 10 per cent of the integrated fluorescence intensity. Optical excitation of the fluorescence is achieved most efficiently by pumping into the absorption band near 17,000 cm^{-1}. Using an AH6-type high-pressure mercury discharge lamp in a manner described in Section VIII, Johnson, *et al.*,[4,22] were able to obtain CW laser action from a water-cooled crystal.

[15] Z. J. Kiss and R. C. Duncan, Jr., "Optical maser action in $CaF_2:Tm^{2+}$," PROC. IRE (*Correspondence*), vol. 50, p. 1532–1533; June, 1962.

[16] The quantum efficiency is defined here as the probability that the absorption of a pump photon will result in the emission of a photon at ν_{12}. Having $t_2 \sim t_{spont}$ is a necessary condition for high quantum efficiency.

[17] See, for instance, D. S. McClure, "Electronic spectra of molecules and ions in crystals. Part II—Spectra of ions in crystals," in "Solid State Physics," F. Seitz and D. Turnbull, Eds., Academic Press, New York, N. Y., vol. 9, pp. 400–459.

[18] See, for instance, "American Institute of Physics Handbook," McGraw-Hill Book Co., Inc., New York, N. Y.; 1957. See especially Sec. 7-58.

[19] G. H. Dieke and L. A. Hall, "Fluorescent lifetimes of rare earth salts and ruby," *J. Chem. Phys.*, vol. 27, pp. 464–467; August, 1957.

[20] E. H. Carlson and G. H. Dieke, "The state of the Nd^{3+} ion as derived from the absorption and fluorescence spectra of $NdCl_3$ and their Zeeman effects," *J. Chem. Phys.*, vol. 34, pp. 1602–1609; May, 1961.

[21] L. F. Johnson and K. Nassau, "Infrared fluorescence and stimulated emission of Nd^{3+} in $CaWO_4$," PROC. IRE (*Correspondence*), vol. 49, pp. 1704–1706; November, 1961.

[22] L. F. Johnson, G. D. Boyd, K. Nassau, and R. R. Soden, "Continuous operation of a solid state optical maser," *Phys. Rev.*, vol. 126, pp. 1406–1409; May 15, 1962.

Using dielectric mirrors Johnson[23] recently obtained ~0.5-watt output.

The strong infrared emission at 2.36 μ from $CaF_2:Dy^{2+}$ is due, as shown in Fig. 3, to a $^5I_7 \rightarrow {}^5I_8$ transition terminating ~35 cm^{-1} above the ground state. The fluorescence and pulsed laser emission in this system were first discovered by Kiss and Duncan.[24] Continuous operation of a $CaF_2:Dy^{2+}$ laser was achieved by Kiss and Duncan,[25] Johnson[26] and Yariv.[27] The very efficient pumping of this laser is due principally to a 4f-5d band near 11,000 cm^{-1} (~0.9 μ) which coincides with a rich emission region of the xenon discharge (~6 per cent to 10 per cent of total output). Using a compact arc xenon discharge lamp Yariv[27] obtained a power output of 0.3 watt with 700-watt input at 77°K. The threshold for CW operation under the same conditions was 100 watts which is the lowest CW threshold reported for a solid system.

Iron (3d) Transition Ions in Crystals

The available optical data of the 3d series is well summarized.[17] The 3d electrons are exposed to the crystal field and the position and nature of the levels are markedly different from the free ion case. This, as noted earlier, is the main reason why a different nomenclature is adopted in describing the spectra.

The only member of this group in which laser action has been observed[2] is Cr^{3+} incorporated into Al_2O_3 (ruby). The theoretical understanding of the ruby spectrum is due mostly to the work of Tanabe and Sugano.[28] The demonstration of laser action in this crystal by Maiman[2] followed a detailed investigation of the pumping and fluorescence dynamics.[29] Our understanding of the laser action in ruby is, consequently, more complete than that of any other laser system.

The emission spectrum at 77°K consists of two lines: R_1 at 6934 Å which is shown in Fig. 3 as originating from the $\bar{E}$ level and the R_2 line (not shown) at 6919 Å originating from the $2\bar{A}$ level. Both lines terminate on the ground state $^4A_2$. The laser emission usually observed is due to the R_1 transition at 6934 Å. The fluorescence linewidth is ~11 cm^{-1} at 300°K and ~0.1 cm^{-1} at 77°K. The radiative lifetime of the $\bar{E}$ (^2E) metastable level is 2.9 msec.[29] The useful excitation is due mostly to absorption by the $^4F_2$ and $^4F_1$ bands and the quantum efficiency is near unity. The critical inversion for oscillation in the R_2 transition is slightly larger than that of the R_1 emission because of a slightly larger t_{spont} and because of the rapid thermalization which causes the population of $2\bar{A}$ to be smaller than that of $\bar{E}$. Consequently, oscillation at R_1 normally prevents oscillation at R_2 from taking place. However, oscillation at R_2 has been observed by using frequency sensitive mirrors which raise the threshold for the R_1 transition.[30]

If we assume a ruby resonator with $\alpha = 0.02$ (2 per cent loss per pass) and $L = 10$ cm we get $t_{photon} \sim 2 \times 10^{-8}$ sec.

Using the equations developed in Section IV and the following data:

$$\Delta\nu = 11 \text{ cm}^{-1}$$

$$t_{spont} \sim 3 \times 10^{-3} \text{ sec}$$

refractive index ~1.76

$$\nu = 14{,}418 \text{ cm}^{-1}$$

$$\left.\begin{aligned} g_1 &= g(^4A_2) = 4 \\ g_2 &= g(\bar{E}) = 2 \end{aligned}\right\} \textit{i.e.,}\ \frac{g_1}{g_2} = 2$$

to calculate the critical inversion for ruby at room temperature we get

$$N(\bar{E}) - N(^4A_2)\left(\frac{2}{4}\right) \sim 10^{17}(V)$$

at 290° $N(2\bar{A})/N(\bar{E}) = 0.87$. (This is the Boltzmann ratio for $T = 290°$ and $\Delta E = 29$ cm^{-1}.) Assuming a typical density of 2×10^{19} atoms/c.c. for pink ruby we get

$$N(\bar{E}) + N(^4A_2) + N(2\bar{A}) = 2 \times 10^{19}V.$$

This results in

$$\frac{N(2\bar{A})}{V} = 0.454 \times 10^{19}$$

$$\frac{N(\bar{E})}{V} = 0.522 \times 10^{19}$$

$$\frac{N(^4A_2)}{V} = 1.024 \times 10^{19},$$

i.e., in order to obtain an inversion of 10^{17} atoms/c.c. we have to maintain $\sim 5 \times 10^{18}$ atoms/c.c in the excited

[23] L. F. Johnson, "Optical Maser Characteristics of Rare Earth Ions in Crystals," to be published.
[24] Z. J. Kiss and R. C. Duncan, "Optical Maser Action in $CaF_2:Dy^{2+}$," post deadline paper, Spring Meeting of the American Physical Society, Washington, D. C.; April, 1962.
[25] Z. J. Kiss and R. C. Duncan, "Pulsed and continuous optical maser action in $CaF_2:Dy^{2+}$," PROC. IRE (*Correspondence*), vol. 50, pp. 1531–1532; June, 1962.
[26] L. F. Johnson, "Continuous operation of the $CaF_2:Dy^{2+}$ optical maser," PROC. IRE (*Correspondence*), vol. 50, pp. 1691–1692; July, 1962.
[27] A. Yariv, "Continuous operation of a $CaF_2:Dy^{2+}$ optical maser," PROC. IRE (*Correspondence*), vol. 50, pp. 1699–1700; July, 1962.
[28] S. Sugano and Y. Tanabe, "Absorption spectra of Cr^{3+} in Al_2O_3," *J. Phys. Soc. Japan*, vol. 13, pp. 880–910; August, 1958.
[29] T. H. Maiman, "Optical and microwave optical experiments in ruby," *Phys. Rev. Letter*, vol. 4, pp. 564–566; June 1, 1960.
[30] F. J. McClung, S. E. Schwarz, and F. J. Meyers, "R_2 line optical maser action in ruby," *J. Appl. Phys.*, vol. 33, pp. 3139–3141; October, 1962.

state. The increase in threshold power resulting from three-level operation is thus ~50. Note that, because of the larger degeneracy of the ground state, laser action obtains with $N_2 < N_1$ [$N_2 = N(\bar{E})$, $N_1 = N(^4A_2)$].

Continuous operation of a ruby laser of 77°K has been achieved by Nelson and Boyle[5] with a power output of a few milliwatts.

Actinide (5f) Series Ions in Crystals

This atomic series is similar to the 4f series in having its unpaired 5f electrons partially shielded (by 6s and 6p electrons). This shielding is not as effective as that of the rare earth ions, and the departures of the energy levels from the free ion positions (crystalline Stark effect) is more pronounced. Only thorium (Th) and uranium (U) occur naturally as long-lived isotopes; the other elements are radioactive. Laser action of trivalent uranium in CaF_2 was first reported by Sorokin and Stevenson[31] and CW laser emission by Boyd, *et al.*[6] The first spectroscopic studies of $CaF_2:U^{3+}$ are those of Galkin and Feofilov.[32] The pertinent energy levels are shown in Fig. 3 and are taken from Boyd, *et al.*[6] The laser emission at 2.61 μ is due to a transition from a level belonging to $^4I_{11/2}$ to one belonging to the $^4I_{9/2}$ Stark split multiplet which is 609 cm^{-1} from the ground state. This separation is large enough so that four-level operation obtains for temperatures below ~100°K. The lifetime t_2 of the metastable level is 130 μsec and is radiative, *i.e.*, $t_2 \approx t_{spont}$.

The useful absorption is due principally to three weak infrared bands near 11,000 cm^{-1}.[6] The threshold for pulsed operation is ~1.0 joules.[33] Threshold values as low as 250 watts were obtained for continuous operation at 77°K with the use of a xenon compact arc lamp in an elliptic pumping geometry.[33] By increasing the lamp input to ~700 watts a power output of ~1 watt was obtained from a crystal with optimal dielectric mirrors. The crystal exhibits laser oscillation, on a pulse basis, at a number of other wavelengths between 2.2 μ and 2.6 μ. These oscillations correspond to other $^4I_{11/2} \rightarrow {}^4I_{9/2}$ transitions which have been determined by Porto and Yariv.[34]

Glass Lasers

Pulsed laser action in a number of glasses has been reported in Nd,[35] Yb,[36] Ho,[37] and Gd.[38] The lack of a unique and well-defined crystalline surrounding for the individual active atoms incorporated into the glass matrix causes the emission lines to be somewhat broader. The laser thresholds for glass lasers (see Table I) have been found to run higher than their crystalline counterparts. The oscillation wavelength of 3125 Å observed in Gd[38] is the only ultraviolet laser emission reported to date. A listing of the reported laser emissions in glasses is included in Table I.

Semiconductor Lasers

The most recent additions to the laser family are the semiconductor lasers reported, independently, by Hall, *et al.*,[39] and by Nathan, *et al.*[40]

The laser emission at $\lambda = 0.842$ μ was observed in forward-biased, highly doped (degenerate) GaAs *p-n* junctions cooled to 77°K. The radiation which originates in the vicinity of the junction is due to transitions of injected electrons (and holes) between the low-lying levels of the conduction band (or donor lying just below the conduction band edge) and the uppermost levels of the valence band (or shallow acceptor levels). The frequency of the emitted radiation corresponds, consequently, very nearly to the band gap energy.

Because of the degeneracy of the diode the electron levels just below the forbidden gap on the *p* side are empty while those just above the gap on the *n* side are full. Consequently, no photons with energies $h\nu \approx E_{gap}$ can be absorbed by interband transitions and the equivalent of four-level laser operation obtains. The main loss mechanism is free-carrier absorption, but this obviously is more than compensated for by the strong radiative transitions.

The quantum efficiencies reported are ~1, *i.e.*, the injection of each electron (or hole) results in the emission of a photon. This has to be constrasted with the over-all efficiency of <1 per cent reported for optically pumped lasers (see Section IX).

The current densities at threshold for 77°K operation are ~8500 A/cm^2. The considerable heating accompanying such a large current density made it necessary to operate the lasers on a pulse basis, with pulse widths of up to 20 μsec.

[31] P. P. Sorokin and M. J. Stevenson, "Stimulated infrared emission from trivalent uranium," *Phys. Rev. Lett.*, vol. 5, pp. 557–559; December, 1960. Also, "Stimulated Emission from $CaF_2:U^{3+}$ and $CaF_2:Sm^{2+}$," in "Advances in Quantum Electronics," J. R. Singer, Ed., Columbia University Press, New York, N. Y., and London, England, pp. 65–77; 1961.

[32] L. N. Galkin and P. P. Feofilov, "The luminescence of trivalent uranium," *Dokl. Akad. Nauk SSSR*, vol. 114, pp. 745–747; January 1957. (Trans. in *Soviet Phys.-Doklady*, vol. 2, pp. 255–257; May-June, 1957.) Also, L. N. Galkin and P. P. Feofilov, *Optics and Spectroscopy*, vol. 1, pp. 492–495; April, 1959.

[33] A. Yariv, "Power Output and Optimum Coupling in Continuous Solid State Lasers," to be published.

[34] S. P. S. Porto and A. Yariv, "Low Lying Energy Levels and Comparison of Maser Action of Uranium in CaF_2, SrF_2, BaF_2," to be published.

[35] E. Snitzer, "Optical maser action of Nd^{3+} in a barium crown glass," *Phys. Rev. Lett.*, vol. 7, pp. 444–446; December, 1961.

[36] H. W. Etzel, H. W. Gandy, and R. J. Ginther, "Stimulated Emission of Infrared Radiation from Ytterbium Activated Silicate Glass," Naval Research Lab., Washington, D. C., NRL Progress Repts.; pp. 27–28; February, 1962.

[37] H. W. Gandy, R. J. Ginther, "Stimulated emission from holmium activated silicate glass," PROC. IRE (*Correspondence*), vol. 50, pp. 2113–2114; October, 1962.

[38] H. W. Gandy and R. J. Ginther, "Stimulated emission of ultraviolet radiation from gadolinium activated glass," *Appl. Phys. Lett.*, vol. 1, pp. 25–27; September, 1962.

[39] R. N. Hall, G. E. Fenner, J. D. Kingsley, T. J. Soltys, and R. O. Carlson, "Coherent light emission from GaAs junctions," *Phys. Rev. Lett.*, vol. 9, pp. 366–367; November 1, 1962.

[40] M. I. Nathan, W. P. Dumke, G. Burns, F. H. Dill, and G. Lasher, "Stimulated emission of radiation from GaAs p-n junctions," *Appl. Phys. Lett.*, vol. 1, pp. 62–64; November, 1962.

TABLE I*

PROPERTIES OF SOLID LASER MATERIALS†

Laser Material	Output Wavelength (microns)	Operating Mode and Temperature	t_{spont} m sec	Pulse Threshold in Joules and Temperature	Useful Absorption Regions (Microns)	Position of Terminal Level (E_1) (cm^{-1})	Laser Transition	Remarks	References
$Cr^{3+}:Al_2O_3$ (ruby)	0.6934 (R_1, 77°)	cw (77) pulsed (350)	3	~800 (77)	0.5–0.6 0.32–0.44	0	$^2E(\bar{E}) \rightarrow {}^4A_2$	"spiking" observed in both pulsed and CW operation	2,41
10^{19} atoms/cc	0.6929 (R_2, 290°)	pulsed			0.5–0.6 0.32–0.44	0	$^2E(2\bar{A}) \rightarrow {}^4A_2$		30
$Cr^{3+}:Al_2O_3$ $n \sim 10^{23}$	0.701, 0.704	pulsed (77)				~100		due to paired chromium ions	42,43
$U^{3+}:CaF_2$	2.613	pulsed (300) CW (~100)	0.13 (77)	1 (77)	~0.9	609	$^4I_{11/2} \rightarrow {}^4I_{9/2}$	"spiking" present in pulsed but not in CW operation. Pulsed emission also observed in BaF_2 at 2.556 μ and in SrF_2 at 2.472 μ, 2.408 μ	6,31,33,34,44–46
	2.438	pulsed (77)							
	2.511	pulsed (77)		6 (77)					
	2.223	pulsed (77)		2000(77)		0			
$Nd^{3+}:CaWO_4$	1.065	CW (300)		~1 (77)	0.57–0.6	~2000	$^4F_{3/2} \rightarrow {}^4I_{11/2}$	"spiking" present in pulsed but not in CW operation. Laser emission from Nd^{3+} also observed in $SrMO_4$, $SrWO_4$, $CaMO_4$, $PbMO_4$, CaF_2, SrF_1, BaF_2, and LaF_3	20,21,47–49
	1.063	pulsed		14 (77)					
	1.066	pulsed	~0.1 (77)	6 (77)					
	1.058	pulsed		80 (77)					
	1.064	pulsed		7 (77)					
Nd^{3+}:Glass	1.06	pulsed (300)		~50		~2000	$^4F_{3/2} \rightarrow {}^4I_{11/2}$		35
$Pr^{3+}:CaWO_4$	1.047	pulsed (77)	0.05 (77)	15 (77)	0.45–0.5	377	$^1G_4 \rightarrow {}^3H_4$	Pulsed laser emission of Pr^{3+} was also detected in $SrMO_4$	50
$Dy^{2+}:CaF_2$	2.36	CW (90)	~10 (77)	20 (77)	0.8–1.0	35	$^5I_7 \rightarrow {}^5I_8$	"spiking" in pulsed operation but not in continuous	24–27
$Tm^{3+}:CaWO_4$	1.911	pulsed (77)		60 (77)	{0.46–0.48	~325	$^3H_4 \rightarrow {}^3H_6$	1.918 μ emission also observed Laser emission also observed in SrF_2	51
	1.916	pulsed (77)		73 (77)	{1.7–1.8				
$Er^{3+}:CaWO_4$	1.612	pulsed (77)		800 (77)	0.38 0.52	375	$^4I_{13/2} \rightarrow {}^4I_{15/2}$		52
$Ho^{3+}:CaWO_4$	2.046	pulsed (77)		80 (77)	0.44–0.46	~230	$^5I_7 \rightarrow {}^5I_8$		49,53
	2.059	pulsed (77)		250 (77)					
$Tm^{2+}:CaF_2$	1.116	pulsed (~4)	4	50 (4)	0.28–0.34 0.39–0.46 0.53–0.63	0	$^2F_{5/2} \rightarrow {}^2F_{7/2}$		15
$Sm^{2+}:CaF_2$	0.708	pulsed (20)	0.002	0.01 (20)	0.425–0.5 0.59–0.65	263	$^5D_0 \rightarrow {}^7F_1$	No "spiking" in pulsed operation. Laser action at 0.6969 μ also observed in $SrF_2:Sm^{2+}$	31,54
Yb^{3+}:Glass	1.015	pulsed (77)	1.5	1300	~0.91 ~0.95 ~0.98		$^2F_{5/2} \rightarrow {}^2F_{7/2}$		36
Gd^{3+}:Glass	0.3125	pulsed (77)	4(300)		0.274 0.277		$^6P_{7/2} \rightarrow {}^8S_{7/2}$		38
Ho^{3+}:Glass	$\lambda > 1.95$ μ	pulsed (77)	~0.7 (77)	3600 (77)	0.44–0.46		$^5I_7 \rightarrow {}^5I_8$		37

* Tables II, and III are taken from Patel, *et al.*,[55] aud Faust, *et al.*[56]

† The host crystal in which the best laser results were obtained is discussed in detail. Other host crystals are listed in the "Remarks" column. The temperatures quoted are in °K.

[41] R. J. Collins, D. F. Nelson, A. L. Schawlow, W. Bond, C. G. B. Garrett, and W. Kaiser, "Coherence, Narrowing, Directionality, and Relaxation Oscillations in the Light Emission from Ruby," *Phys. Rev. Lett.*, vol. 5, pp. 303–305; October, 1960.

[42] A. L. Schawlow, D. L. Wood, and A. M. Clogston, "Electronic spectra of exchange-coupled ion pairs in crystals," *Phys. Rev. Lett.*, vol. 3, pp. 271–273; September, 1959.

[43] A. L. Shawlow and H. E. Devlin, "Simultaneous optical maser action in two ruby satellite lines," *Phys. Rev. Lett.*, vol. 6, pp. 96–98; February, 1961. I. Weider and L. R. Sarles, "Stimulated optical emission from exchange-coupled ions of Cr^{+++} in Al_2O_3," *Phys. Rev. Lett.*, vol. 6, pp. 95–96; February, 1961.

[44] H. A. Bostik and J. R. O'Connor, "Infrared oscillations from $CaF_2:U^{+3}$ and $BaF_2:U^{+3}$ masers," PROC. IRE (*Correspondence*), vol. 50, pp. 219–220; February, 1962.

[45] S. P. S. Porto and A. Yariv, "Excitation, relaxation and optical maser action at 2.407 μ in $SrF_2:U^{3+}$," PROC. IRE (*Correspondence*), vol. 50, pp. 1543–1544; June, 1962.

[46] S. P. S. Porto and A. Yariv, "Optical maser action in $BaF_2:U^{3+}$," PROC. IRE (*Correspondence*), vol. 50, pp. 1542–1543; June, 1962.

[47] L. F. Johnson and R. R. Soden, "Optical maser characteristics of Nd^{3+} in $SrMO_4$," *J. Appl. Phys.* (*Correspondence*), vol. 33, pp. 757; February, 1962.

[48] L. F. Johnson, "Optical maser characteristics of Nd^{3+} in CaF_2," *J. Appl. Phys.* (*Correspondence*), vol. 33, pp. 756; February, 1962.

[49] L. F. Johnson, "Optical Maser Characteristics of Rare Earth Ions in Crystals," to be published.

[50] A. Yariv, S. P. S. Porto, and K. Nassau, "Optical maser emission from trivalent praseodymium in calcium tungstate," *J. Appl. Phys.*, vol. 33, pp. 2519–2521; August, 1962.

S. P. S. Porto, R. R. Soden, and A. Yariv, "Optical maser emission in $SrMO_4:Pr^{3+}$ at 1.04 μ," unpublished.

[51] L. F. Johnson, G. D. Boyd, and K. Nassau, "Optical maser characteristics of Tm^{3+} in $CaWO_4$," PROC. IRE (*Correspondence*), vol. 50, pp. 86–87; January, 1962.

[52] Z. J. Kiss and R. C. Duncan, Jr., "Optical maser action in $CaWO_4:Er^{3+}$," PROC. IRE (*Correspondence*), vol. 50, p. 1531; June, 1962.

[53] L. F. Johnson, G. D. Boyd, and K. Nassau, "Optical maser characteristics of Ho^{3+} in $CaWO_4$," PROC. IRE (*Correspondence*), vol. 50, pp. 87–88; January, 1962.

[54] W. Kaiser, C. G. B. Garrett, and D. L. Wood, "Fluorescence and optical maser effects in $CaF_4:Sm^{++}$," *Phys. Rev.*, vol. 123, pp. 766–776; August, 1961.

D. L. Wood and W. Kaiser, "Absorption and fluorescence of Sm^{2+} in CaF_2, SrF_2, and BaF_2," *Phys. Rev.*, vol. 126, pp. 2079–2080; June, 1962.

[55] C. K. N. Patel, W. R. Bennett, Jr., W. L. Faust, and R. A. McFarlane, "Infrared spectroscopy using stimulated emission techniques," *Phys. Rev. Lett.*, vol. 9, pp. 102–104; August 1, 1962.

[56] W. L. Faust, R. A. McFarlane, C. K. N. Patel, and C. G. B. Garrett, "Gas Maser Spectroscopy in the Infrared," to be published.

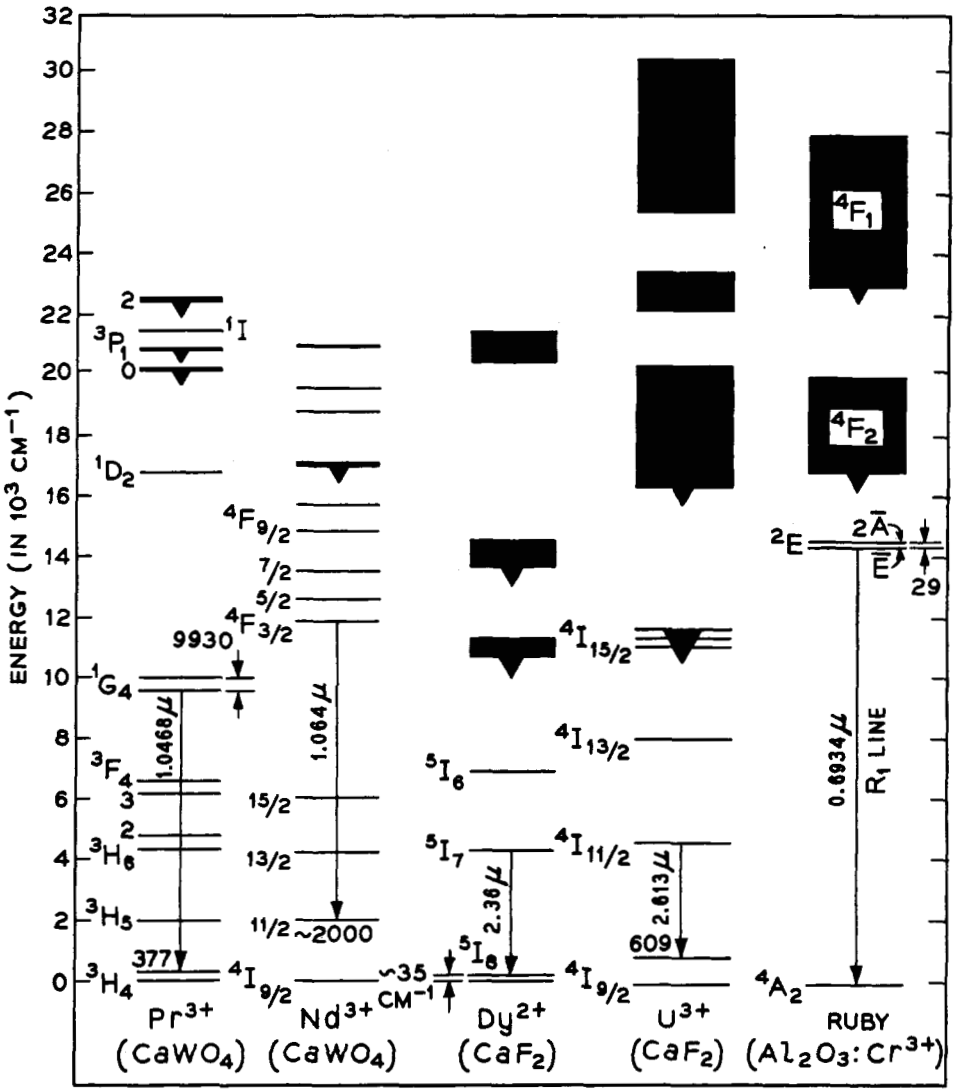

Fig. 3—Energy-level diagrams of $CaWO_4:Pr^{3+}$, $CaWO_4:Nd^{3+}$, $CaF_2:dy^{2+}$, $CaF_2:U^{3+}$ and $Al_2O_3:Cr^{3+}$. The dark triangles indicate useful absorption bands (or levels).

Gas Lasers

The first CW laser and also the first gas laser was the He-Ne laser of Javan, *et al.*[3] Inversion in the 2S-2p transitions of Ne resulted in oscillation at a number of frequencies around 1.15 μ. The operation of this laser can be explained with the aid of Fig. 4 (page 15). An RF (or dc) discharge is established in the gas mixture containing, typically, 1.0-mm Hg of He and 0.1 mm of Ne. The energetic electrons in the discharge excite helium atoms into a variety of excited states. In the normal cascade of these excited atoms down to the ground state, many collect in the long-lived metastable state 2^3S. It is primarily these excited metastable helium atoms which then pump the neon atoms up into the upper maser levels labeled 2S. They do this by colliding with unexcited neon atoms, and exchanging energy with them. The small difference in energy, about 0.04 volt in the case of the highest of the neon 2S levels, is taken up by kinetic energy in the colliding atoms. Thus the helium atoms act as a funnel to convey the broad band of excitation (from the electrons) into a few sets of neon levels. The terminal laser level, or rather the set of possible terminal laser levels labeled 2p, decay radiatively to the metastable 1s state in a time (0.01 μsec) which is much shorter than the time for spontaneous decay of the 2S down to the 2p levels (0.1 μsec), so the conditions necessary for maser action are indeed satisfied.

There are a couple of subsidiary but yet rather important points which should be made in connection with this scheme. The first is that direct excitation of neon atoms by the electrons in the discharge occurs, and this tends to reduce the inverted population in the laser transition because it provides less discriminant

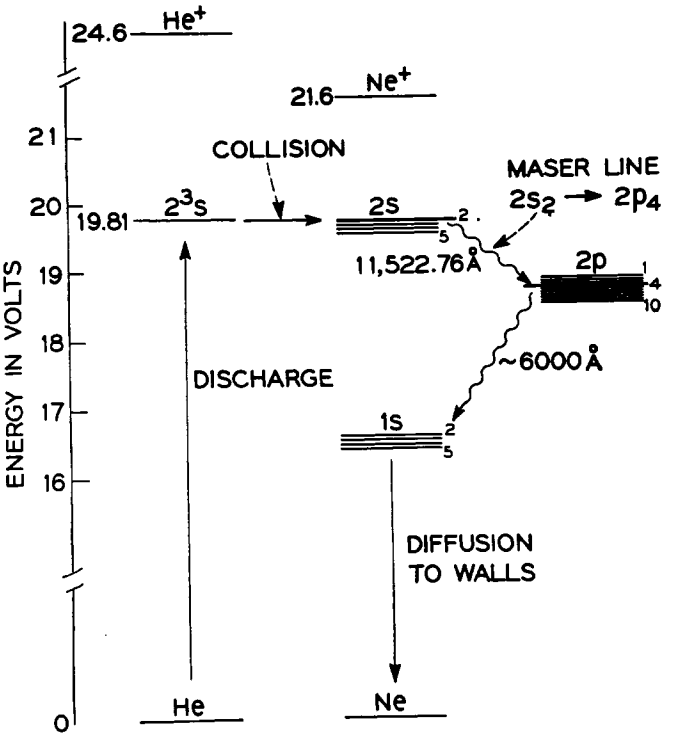

Fig. 4—Energy-level diagram for He and Ne.

excitation of the upper levels. This is why the neon density should be kept considerably below the helium density in the tube. The second is that since the 1S level of neon is also metastable, its population tends to build up as the pumping continues. If the 1S-level population becomes too high the photons emitted by the decaying 2p atoms have a finite chase of re-exciting 1s atoms before they escape from the gas. This process is called radiation trapping, and has the effect of increasing the lifetime of the 2p states, which again tends to reduce the inverted population difference. If the mixture of gases is free from other impurities, then the only way the 1S atoms can decay to the ground state is by colliding with the walls of the gas container. For this reason the gain has been found to be inversely proportional to the tube diameter. Table II summarizes findings by McFarlane, *et al.*,[57] and by White and Rigden[58] and lists all the 2S→2p transitions in which oscillations have been observed. The Paschen notation is used to label the transitions. In addition to these White and Rigden[60] obtained visible laser emission at 6328 Å which is due to the $3S_2 \rightarrow 2p_4$ transition in Ne.

The pumping in this case is again due to a near-energy coincidence between the 2^1S metastable level in He and an excited metastable ($3S_2$) in Ne.

Patel, *et al.*,[55] obtained a variety of oscillations between $\lambda = 1.6\,\mu$ and $\lambda = 2.2\,\mu$ in pure He, Ne, Ar, and Kr. The observed oscillations and the corresponding transitions are listed in Table III. The Racah notation[18] is employed except for the He 7^3D-4^3P transition.

TABLE II

OBSERVED TRANSITIONS IN THE HE-NE LASER (PASCHEN NOTATION)

λ-microns	Transition	Reference
1.0801	$2S_3$-$2p_7$	57
1.08475	$2S_2$-$2p_6$	57
1.11461	$2S_4$-$2p_8$	57
1.11806	$2S_5$-$2p_9$	3
1.13936	$2S_5$-$2p_8$	57
1.14123	$2S_2$-$2p_5$	58
1.15259	$2S_2$-$2p_4$	3
1.16047	$2S_2$-$2p_3$	58
1.16173	$2S_3$-$2p_5$	3
1.17700	$2S_2$-$2p_2$	57
1.19882	$2S_3$-$2p_2$	3
1.20696	$2S_5$-$2p_6$	3
1.52349	$2S_2$-$2p_1$	57
3.39	3S -2p	59
	Visible Transition	
0.6328	$3S_2$-$2p_4$	60

[57] R. A. McFarlane, C. K. N. Patel, W. R. Bennett, Jr., and W. L. Faust, "New helium-neon optical maser transitions," PROC. IRE (*Correspondence*), vol. 50, pp. 2111–2112; October, 1962.

[58] A. D. White and J. D. Rigden, "Simultaneous gas maser action in the visible and infrared," PROC. IRE (*Correspondence*), vol. 50, pp. 2366–2367, November, 1962.

[59] A. L. Bloom, W. E. Bell, and R. C. Rempel, post deadline paper, American Physical Society Meeting, Seattle, Washington, August, 1962.

[60] A. D. White and J. D. Rigden, "Continuous gas maser operation in the visible," PROC. IRE (*Correspondence*), vol. 50, p. 1697; July, 1962.

TABLE III
THE OBSERVED TRANSITIONS IN THE HE, NE, AR, KR AND XE LASERS (RACAH NOTATION)

Gas	λ_{air} (microns)	Transition	Pressure (mm Hg)	Remarks
Helium	2.0603	7^3D-4^3P	8	Strong
Neon	2.1019	$4d'[5/2]_3^0$-$4p[3/2]_2$	0.2	
Argon	1.618	$5s[3/2]_2^0$-$4p'[3/2]_2$	0.05	
	1.694	$3d[3/2]_1^0$-$4p[3/2]_2$	0.035	
	1.793	$3d[1/2]_1^0$-$4p[3/2]_2$ $3d[1/2]_0^0$-$4p[3/2]_1$	0.035	
	2.0616	$3d[3/2]_2^0$-$4p'[3/2]_2$	0.035	
Krypton	1.690	$4d[1/2]_1^0$-$5p[1/2]_1$	0.07	
	1.694	$4d[5/2]_2^0$-$5p[3/2]_1$	0.05	
	1.784	$4d[1/2]_0^0$-$5p[1/2]_1$	0.07	
	1.819	$4d'[5/2]_2^0$-$5p'[3/2]_2$	0.07	
	1.921	$8s[3/2]_1^0$-$6p[5/2]_2$	0.035	
	2.116	$4d[3/2]_2^0$-$5p[3/2]_1$	0.035	
	2.189	$4d[3/2]_2^0$-$5p[3/2]_2$	0.035	

Gas	λ_{vac}	Transition	Xe	He	Remarks
Xenon	2.0268	$5d[3/2]_1^0$-$6p[3/2]_1$	0.02	5	Very strong Gain~4.5 db/m
	2.3200	$5d[5/2]_3^0$-$6p[5/2]_2$			Very weak
	2.6276	$5d[5/2]_2^0$-$6p[5/2]_2$			
	2.6518	$5d[3/2]_1^0$-$6p[1/2]_0$	0.02	1	Strong
	2.6608	$5d'[3/2]_1^0$-$6p'[1/2]_0$			
	3.1078	$5d[5/2]_3^0$-$6p[3/2]_2$			Very weak
	3.3676	$5d[5/2]_2^0$-$6p[3/2]_1$	0.01	1	Strong
	3.435	$9d[7/2]_3^0$-$8p[3/2]_2$			
	3.5080	$9d[7/2]_3^c$-$6p[5/2]_2$	0.01	1	Very strong
	3.6798	$5d[1/2]_1^0$-$6p[1/2]_1$			Weak
	3.6859	$5d[5/2]_2^0$-$6p[3/2]_2$	0.04	0.3	Strong
	3.8697	$5d'[5/2]_3^0$-$6p'[1/2]_2$			
	3.8950	$5d[7/2]_3^0$-$6p[5/2]_3$			Very weak
	3.9966	$5d[1/2]_0^0$-$6p[1/2]_1$	0.01	1	Strong
	4.1527	$5d'[5/2]_2^0$-$6p[5/2]_2$			
	4.6109	$5d'[3/2]_2^0$-$6p'[1/2]_1$			
	5.5754	$5d[7/2]_4^0$-$6p[5/2]_3$	0.01	zero	Very strong
	7.3167	$5d[3/2]_2^0$-$6p[3/2]_1$			
	9.0065	$5d[3/2]_2^0$-$6p[3/2]_2$			Strong
	9.7029	$5d[1/2]_1^0$-$6p[3/2]_1$			
	12.26	$5d[1/2]_0^0$-$6p[3/2]_1$			
	12.917	$5d[1/2]_1^0$-$6p[3/2]_2$			

Faust, *et al.*,[56] obtained oscillations in an Xe-He system between 1.5 μ and 13 μ. The oscillations which are due to an Xe 5d-6p (Racah notation) are listed in Table III. One of these oscillations, at $\lambda = 2.0268\ \mu$, is also reported in Patel, *et al.*[55] and is quite intense. The gain was measured at 4.5 db/m. The energy levels in Xe are shown in Fig. 5. The 13-μ oscillation in this system is the longest wavelength oscillation reported to date.

The excitation in the He, Ne, Ar, Kr, and Xe lasers is believed to take place via inelastic collisions with the discharge electrons. The collision cross section for excitation of a given level is proportional to the dipole matrix element connecting the excited level with the ground state. Consequently the electron collision process provides a discriminant mechanism for level excitation.

Laser action at 0.8466 μ in oxygen was obtained from Ne-O_2 and Ar-O_2 gas mixtures.[61] The steps involved in the excitation process are the following: An excited state of the Ne or Ar atom ($^3p_1$, $^3p_0$) collides with an unexcited O_2 molecule, thereby elevating it into an excited state. The excited molecule is energetically unstable (repulsive) and splits into a ground state O atom and an excited (3^3P_2) O atom. The laser oscillation at 0.8466 μ is due to a 3^3P_2—3^3S_1 transition of the oxygen atom.

Oscillation at 3.2 μ and 7.2 μ from optically pumped cesium vapor has been achieved by Jacob, *et al.*[62]

The optical resonator used in the gas lasers is a Fabry-Perot interferometer of, typically, 0.5–2 meters length. The earliest versions used plane parallel mirrors inside the gas envelope. A modification due to Rigrod and Kogelnik[63] consists of using spherical mirrors outside the gas envelope which is made possible by two Brewster-angle windows as shown in Fig. 6. The increased flexibility of this arrangement is partly responsible for the ease with which new laser frequencies in gas systems have been discovered recently. The difficulty of obtaining Brewster windows for $\lambda > 2\ \mu$ caused a return to the use of internal reflectors in the recent long λ gas lasers.[56]

Total power output, distributed among a number of longitudinal resonator modes (see Section XIII) of 40 mw in a single transverse mode, is available from some of the transitions near ~1.15 μ in an He-Ne laser.[64] Single-mode operation with an output of ~1.5 mw has been reported recently.[65]

[61] W. R. Bennett, Jr., W. L. Faust, R. A. McFarlane, and C. K. N. Patel, "Dissociative excitation transfer and optical maser oscillation n Ne-O_2 and Ar-O_2 RF discharges," *Phys. Rev. Lett.*, vol. 8, pp. 470–473; June 15, 1962.

[62] S. Jacobs, G. Gould, and P. Rabinowitz, "Coherent light amplification in optically pumped Cs vapor," *Phys. Rev. Lett.*, vol. 8, pp. 415–418; December 1, 1961.

[63] W. W. Rigrod, H. Kogelnik, D. Brangaccio, and D. R. Herriott, "Gaseous optical masers with external concave mirrors," *J. Appl. Phys.*, vol. 33, pp. 743–744; February, 1962.

[64] W. W. Rigrod and A. J. Rustako, "Diffraction Studies with Plane-Parallel Interferometer," to be published.

[65] H. Kogelnik and C. K. N. Patel, "Mode suppression and single frequency operation in gaseous optical masers," PROC. IRE (*Correspondence*), vol. 50, pp. 2365–2366; November, 1962.

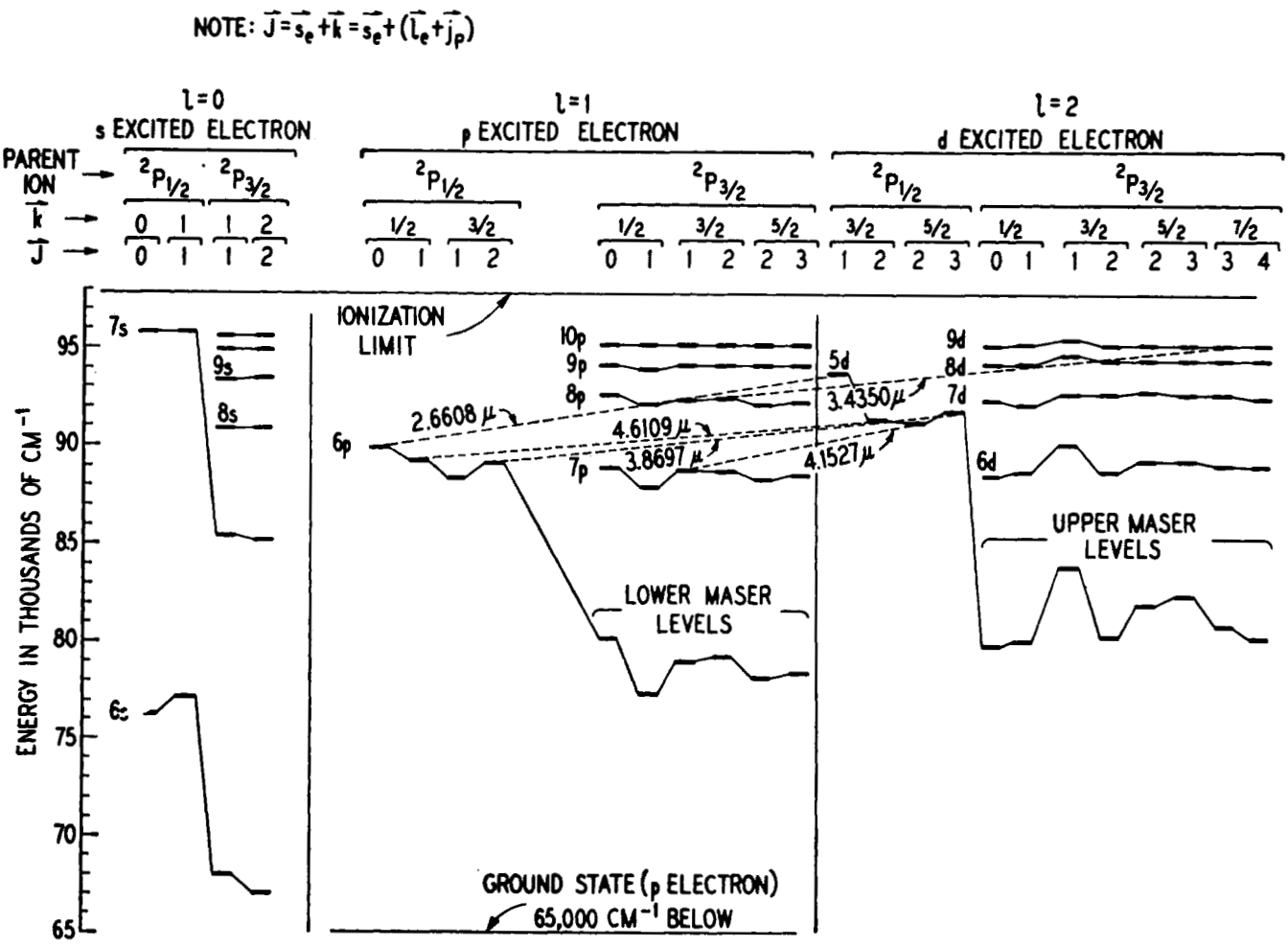

Fig. 5—Energy-level diagram of Xe.

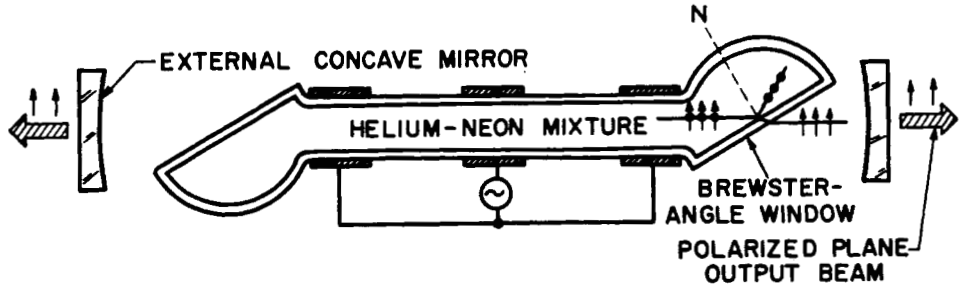

Fig. 6—An experimental setup for gas lasers.

VII. Optical Pumping

In all the solid-state lasers the population inversion has been achieved by illuminating the laser rod with high-intensity lamps. It is, therefore, of interest to combine our knowledge of the critical population inversion with that of the optical characteristics of the crystal and obtain an estimate for the light intensities required to obtain continuous laser action. In doing this we shall use a method first employed by Kaiser, *et al.*[54] If the energy flux per unit wavelength incident on the crystal is $I(\lambda)$, then the power per unit volume absorbed by the crystal is given by

$$P_{abs/V} = \int I(\lambda)K(\lambda)d\lambda, \tag{41}$$

where the attenuation of $I(\lambda)$ is described by $I(\lambda, x) = I(\lambda, 0)e^{-K(\lambda)x}$ and the integration is over the useful absorption ranges.

The equilibrium population of the metastable level established by the pump light is obtained by equating the rate of excitation (atoms per m³ per second) to the rate of decay (assumed radiative)

$$\int \frac{\lambda I(\lambda)K(\lambda)\eta(\lambda)}{hc}\, d\lambda = \frac{N_2}{Vt_{spont}} \tag{42}$$

where V is the volume of the crystal and $\eta(\lambda)$ is the quantum efficiency for pump light at wavelength λ for exciting level 2. It is also assumed that K is small enough so that the decrease in I due to crystal absorption is small. By replacing N_2 by N_{2c} (*i.e.*, N_2 at threshold), which for a four-level laser is equal to ΔN_c, we obtain an expression for the critical light intensity. If we replace I, K, η, by their average values for the useful absorption range $\Delta\lambda$ we can rewrite (42) as

$$\frac{\lambda \bar{I}\bar{K}\bar{\eta}\Delta\lambda}{hc} = \frac{\Delta N_c}{Vt_{spont}}. \tag{43}$$

Numerical Example:

Typical data for 0.1 mole per cent $CaF_2:U^{3+}$ is

$$\lambda_0 = 2.61 \times 10^{-4} \text{ cm}$$
$$L = 3 \text{ cm}$$

refractive index ~ 1.4

$$t_{photon} = 3 \times 10^{-9} \text{ sec (loss per pass} \sim 5 \text{ per cent)}$$
$$\Delta\nu \approx 20 \text{ cm}^{-1}$$
$$t_{spont} = 1.3 \times 10^{-4} \text{ sec.}$$

Using (30) we get

$$\frac{\Delta N_c}{V} = 1.4 \times 10^{15} \text{ atoms/c.c.}$$

which yields for the minimum power density supplied by the pump light P_{fc}/V a value near 0.8 watt/cm³. If we consider this result in (43) and assume that $\bar{K} = 0.3$, $\bar{\eta} \sim 1$, and that the absorption wavelength is $\sim 0.9\ \mu$, we find that the product $\bar{I}\Delta\lambda$, *i.e.*, the total useful light flux at the crystal surface is ~ 8 watts/cm² at threshold.

Using the following data for a typical $CaWO_4:Nd^{3+}$ laser

$$\lambda_0 = 1.064 \times 10^{-4} \text{ cm}$$
$$L = 3 \text{ cm}$$
$$n = 1.9$$
$$t_{photon} = 3.8 \times 10^{-9} \text{ sec (loss per pass} \sim 5 \text{ per cent)}$$
$$\Delta\nu = 7 \text{ cm}^{-1}$$
$$t_{spont} \sim 10^{-4} \text{ sec}$$

we get

$$\frac{\Delta N_c}{V} \sim 5 \times 10^{15} \text{ atoms/c.c.}$$

$$\frac{P_{fc}}{V} = \frac{\Delta N_c h\nu}{Vt_{spont}} \sim 10 \text{ watts/cm}^3.$$

Thus the maintenance of critical inversion in $CaWO_4:Nd^{3+}$ requires approximately ten times [this is mostly because of the ν^3 term in (35)] more power than in $CaF_2:U^{3+}$. The fact that both lasers require similar CW pumping powers[4,6] is, most likely, due to the far stronger absorption of $CaWO_4:Nd^{3+}$ in the useful excitation region near 5800 Å when compared to that of $CaF_2:U^{3+}$ near 0.9 μ. From data supplied by Johnson[23] the average absorption coefficient of $CaWO_4:Nd^{3+}$ in the 5800-Å band can be calculated as $\bar{K} \sim 5$ cm⁻¹. The critical flux $\bar{I}\Delta\lambda$ can then, very roughly, be estimated as being 1 to 3 watts/cm².

These numerical estimates will be compared in Section IX with actual power measurements in $CaWO_4:Nd^{3+}$ and $CaF_2:U^{3+}$ lasers.

If the pumping geometry affords more than one absorption pass for pumping light through the laser rod the critical light flux is even smaller.

VIII. Some Experimental Notes

Detectors

The type of detectors used in the observation of laser signals is dictated mostly by the wavelength region of the signal and the time resolution required. At wavelengths up to $\sim 1.1\ \mu$ conventional photomultipliers are the most suitable. For the 1 to 3 μ region the most suitable detectors are PbS and PbSe photoconductive cells. The former are more sensitive but have longer response times (typical value ~ 0.5 msec) which limits their application for pulse work. PbSe detectors have time constants of the order of 2 to 5 μsec which makes them suitable for pulsed laser detection. Gold-doped germanium photoconductive detectors cooled to ~ 77°K are effective up to 9 μ (with $\tau \approx 1\ \mu$sec) while for longer wavelengths one may use Golay cells and thermocouples (or piles) for detection not requiring fast time response (*i.e.*, CW operation). For fast response at

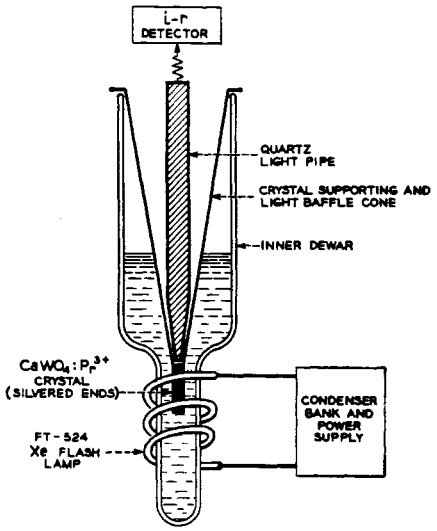

Fig. 7—An experimental setup for pulsed lasers.

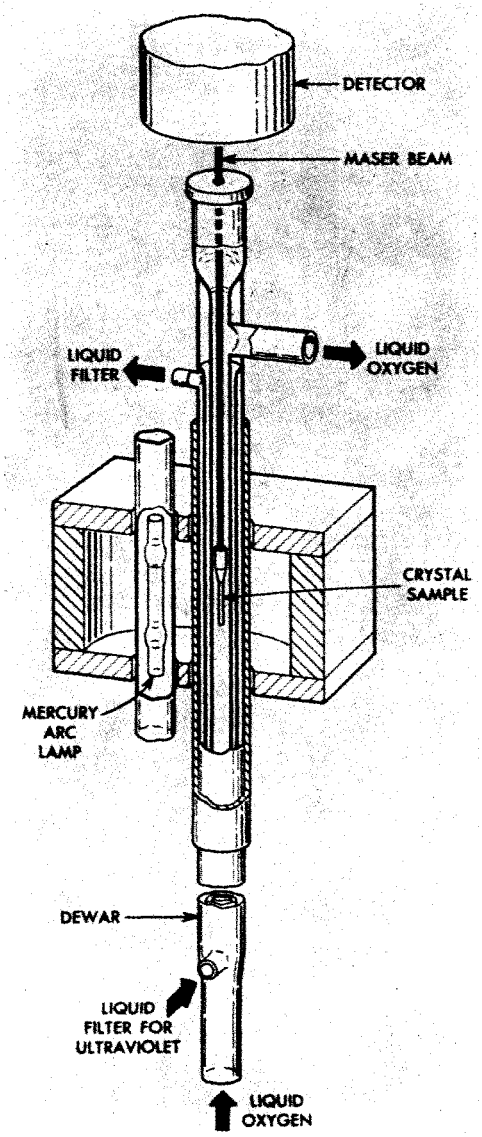

Fig. 8—An experimental setup for CW solid lasers. The cylinder around the dewar is a heat shield which is removed during operation.

$\lambda > 9\,\mu$ we can use photoconductive cells cooled to liquid hydrogen (20°K) and liquid helium (4.2°K) temperatures. A copper-doped germanium cell cooled to 4.2°K can be used up to 30 μ with time resolution of ~ 1 μsec.

Experimental Setups for Laser Action

A typical experimental arrangement used in pulsed laser measurements is shown in Fig. 7. The pulse threshold values reported in Table I and throughout this article refer to such a geometry.

Fig. 8 illustrates an arrangement used to obtain continuous laser action in $CaWO_4:Nd^{3+}$ (Johnson, *et al.*[4]), $CaF_2:U^{3+}$ (Boyd, *et al.*[6]), and $CaF_2:Dy^{2+}$.[26,27] The highly polished elliptic cylinder is used to concentrate the radiation from the discharge lamp, which is placed along one focal axis, onto the laser rod which is placed along the other axis. The crystal is surrounded by a double flow dewar. A flow of a suitable coolant is maintained in the inner dewar space. This coolant keeps the crystal at the proper operating temperature and carries away the heat generated in the crystal by the pump light. The outer annular region of the dewar is used for a flow of liquid filter which absorbs pump radiation not useful in exciting the desired transition. This is very important since most of the heating in lasers such as $CaF_2:U^{3+}$ (Boyd, *et al.*[6]), and $CaF_2:Dy^{2+}$ (Yariv[27]), is due mostly to "useless" radiation which can be avoided. In $CaWO_4:Nd^{3+}$ (Johnson, *et al.*[4]), the presence of ultraviolet radiation in the pumping light was found to induce some new centers which degraded the laser performance.

The lamps most suitable for this geometry are the capillary Hg discharge lamp (the AH6, for example) and compact arc xenon lamps. The former is richer in visible radiation and has been used on $CaWO_4:Nd^{3+}$, while the latter is particularly useful for cases (like $CaF_2:U^{3+}$ and $CaF_2:Dy^{2+}$) requiring infrared pumping.

A novel pumping scheme was used by Nelson and Boyle[5] to obtain continuous laser action in ruby. It is illustrated in Fig. 9. The high-intensity region of a short arc Hg lamp is imaged on the broad base of a trumpet-shaped rod with unity magnification. The cone is made out of sapphire (clear Al_2O_3) while the shank contains a small concentration (1.6×10^{18} atoms/c.c.) of chromium atoms. The light incident on the cone base is trapped by total internal reflection so that intensity at the ruby shank is larger than at the cone base by a factor which is equal to the ratio of the areas. The pumping radiation zig-zags down the rod and after reflection from the far mirror retraces its path, thus increasing the optical path length and consequently the absorption. The increased absorption plus the high intensity were sufficient to maintain CW action at 77°K. The reported output was ~ 4 mw. It should be noted that the end-pumping scheme is especially advantageous for three-level lasers. This is because the concentration of the active atoms must be kept low enough so as to insure uniform pumping over the rod's length. Lowering the

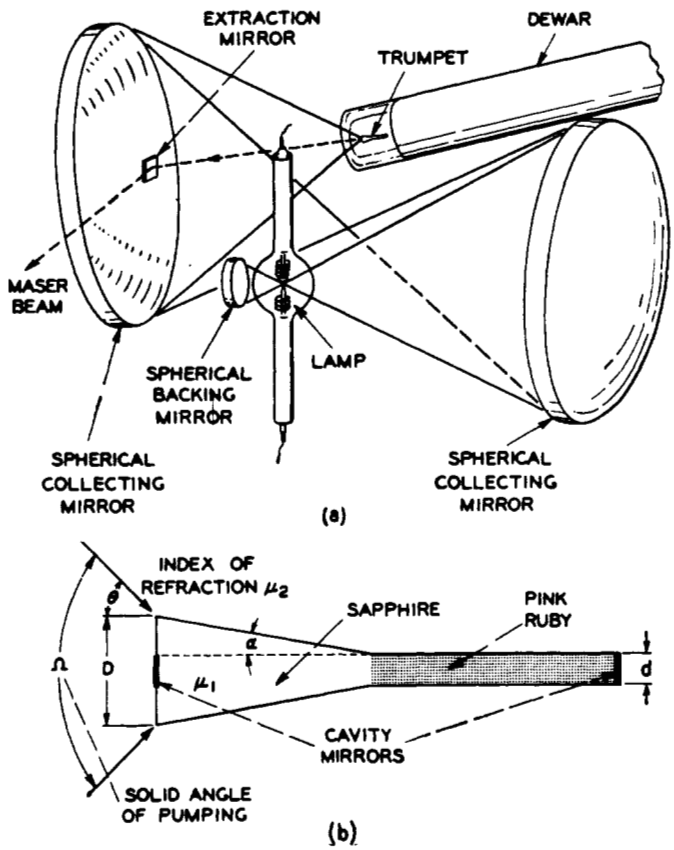

Fig. 9—Ruby CW laser setup.

concentration does not lead to an increase in threshold in three-level lasers (as long as the total population $N_0 \gg \Delta N_c$) but would cause a proportional increase in threshold in four-level lasers.

In Fig. 6 is shown a typical gas laser setup in which Brewster angle windows and external reflectors are used.

Cooling Considerations

Since the reported output from a number of CW solid-state lasers[23,27,38] is ~1 watt and the power dissipated as heat in the crystal rod is at least several times larger, it is clear that if the operating temperature of the crystal is not to rise excessively, an efficient means of carrying away this heat must be employed. The thermal resistance impeding the cooling consists of that of the crystal material itself and of the crystal-coolant barrier layer. Data on thermal conductivity in a number of crystals used in laser applications[66-68] indicate peak thermal conductivities of ~30–100 watts/cm-°K occurring between 10°K and 30°K and a decrease by more than a factor of ten at liquid nitrogen temperature (77°K). As a result the thermal conductivity of the crystal material does not constitute a bottleneck in heat dissipation since only a few degrees of temperature differentials (assuming lateral dimensions of a few millimeters) are sufficient to maintain heat fluxes > 10 watts/cm².

Data on heat transfer through solid-liquid interfaces[69] indicate a maximum of ~10 watts/cm² for immersion cooling in liquid nitrogen. The temperature rise of the crystal above the coolant is ~20°K. The corresponding numbers for water are 100 watts/cm² and 54°K. The situation is improved radically, as shown by Table 16.17 of Grober and Erk[69] by employing a flowing coolant below its boiling temperature (subcooling) which reduces the temperature rise of the crystal and increases the maximum heat transfer compared to the immersion case. Liquid oxygen subcooled to 77°K (normal boiling temperature at atmospheric pressure is 90°K) was used successfully to cool $CaWO_4:Nd^{3+}$ [4] and $CaF_2:U^{3+}$ [6] CW lasers.

DiGiovanni[70] measured a temperature rise of 8°K in $CaF_2:U^{3+}$ and $CaWO_4:Nd^{3+}$ crystals under experimental conditions resembling those prevailing in the CW experiments.[4,6] The crystals were illuminated by an AH6 Hg lamp in an elliptic configuration and cooled by a flow of subcooled liquid oxygen.

IX. Output Power Considerations

A detailed treatment of the power problem in laser oscillators cannot be included in this paper and will be published elsewhere.[33] We shall merely present some of the results and discuss their implication.

Referring again to the laser transition $2 \leftrightarrow 1$ in Fig. 2, let the pumping rate of level 2 be R_2 (atoms/sec) and its lifetime t_2. The corresponding quantities for level 1 are R_1 and t_1. Let the induced transition rate be W_i. Instead of using W_i as given by (22), it is found advantageous to employ a form suggested by (37). If (37) is rewritten as

$$(N_2 - N_1)\left(\frac{n}{pt_{\text{spont}}}\right) \geq \frac{n}{t_{\text{photon}}} \tag{44}$$

where n is the total number of photons in the resonator. It is clear that W_i can be written as

$$W_i = \frac{n}{pt_{\text{spont}}}. \tag{45}$$

A solution of the equilibrium populations N_2 and N_1 under the simultaneous influence of the pumping and

[66] G. A. Slack, "Thermal conductivity of MgO, Al_2O_3, $MgAl_2O_4$, and Fe_3O_4 crystals from 3°K to 300°K," *Phys. Rev.* vol. 126, pp. 427–442; April, 1962. Also "Thermal Conductivity of CaF_2, MnF_2, CoF_2, and ZnF_2," *Phys. Rev.* vol. 122, pp. 1451–1468; June, 1961.

[67] G. K. Chang, J. R. Lankard, P. P. Sorokin, and J. M. Stevenson, "Operation of CaF_2 masers at low temperatures," *Proc. Northeast Electronics Research and Engineering Meeting*, Boston, Mass., pp. 20–21; 1961.,

[68] M. G. Holland, unpublished data on $CaWO_4$:Nd.

[69] H. Gröber and S. Erk, "Fundamentals of Heat Transfer," McGraw-Hill Book Co., Inc., New York, N. Y.; 1961.

[70] A. E. DiGiovanni, "Equipment and Cooling Techniques in the Continuous Operation of Solid State Optical Masers," unpublished.

oscillation fields yields for a case of a four-level laser in which the broadening is assumed to be homogeneous

$$N_2 - N_1 = \frac{R_2\left[1 - \frac{t_1}{t_2}\left(1 + \frac{R_1}{R_2}\right)\right]}{\frac{1}{t_2}[W_i t_2 + 1]} = \frac{R_2'}{\frac{1}{t_2}[W_i t_2 + 1]} \tag{46}$$

where the effective pumping rate R_2' is defined by (46). Assuming $t_2 = t_{\text{spont}}$ and equating (46) to ΔN_c as given by (37) leads to an expression for the power output[33]

$$P = P_{fc}(\text{PR} - 1) = \frac{4\pi^2 h\nu^3 V \Delta\nu}{c^3 t_{\text{photon}}}(\text{PR} - 1) \tag{47}$$

where PR is, according to (47), the factor by which critical pumping is exceeded and is given by

$$\text{PR} = \frac{R_2'}{(p/t_{\text{photon}})}. \tag{48}$$

PR will be referred to as the pumping ratio.

In the case of three-level lasers the power output is given by an expression identical to (47) except that P_{fc} is given by

$$P_{fc} = \frac{N_2 h\nu_{12}}{t_{\text{spont}}}$$

which is the critical fluorescence power for a three-level laser.

Using the numerical data of a typical $CaF_2:U^{3+}$ laser crystal with $V = 0.2$ cm^3 supplied in Section VII we calculated $P_{fc} = 0.8 \times 0.2 = 0.16$ watt. The measured output at 2.61 μ from the same laser at 5×threshold (PR = 5) was ~1 watt with total electric power input of ~1 kw.[33] The linear dependence of the power output on the pumping intensity predicted by (47) was also observed up to PR = 7, which was the maximum pumping strength available. Similar power levels were also reported for $CaWO_4:Nd^{3+}$ [27] and $CaF_2:Dy^{2+}$ [23] lasers. The CW power output from solid lasers is thus seen to be consistent with the theoretical expectations and further improvements will most likely result from the introduction of new or improved pumping techniques and from the discovery of laser materials of superior absorption characteristics.

Let us now calculate the critical inversion and the expected power output for the He-Ne gas laser in a typical 2S-2p transition near one micron. The necessary data are:

$$t_{\text{spont}}^{(2S)} = 10^{-7} \text{ sec}$$
$$\nu = 3 \times 10^{14} \text{ cps}$$
$$L = 1 \text{ m}$$
$$\alpha(\text{loss per pass}) = 10^{-2}$$
$$t_{\text{photon}} = \frac{L}{c\alpha} = 3.3 \times 10^{-7} \text{ sec}$$
$$\Delta\nu(\text{Doppler width}) = 9 \times 10^8 \text{ cps}.$$

Using (30), in its Gaussian form, we get

$$\Delta N_c/V = n_2 - n_1 \sim 2 \times 10^7 \text{ atoms/c.c.}$$

The critical fluorescence power density is

$$\frac{P_{fc}}{V} = \frac{\Delta N_c h\nu}{V t_{\text{spont}}} \sim 7 \times 10^{-5} \text{ watts/cm}^3.$$

Using $V = 100$ cm^3 ($L = 100$ cm, $A = 1$ cm^2) yields

$$P_{fc} \sim 7 \text{ mw}.$$

Rigrod[64] has obtained 40-mw power output from an He-Ne laser at 1.15 μ under experimental conditions similar to those used in the above example. This would indicate, according to (47) and the above estimate of P_{fc}, a pumping ratio PR~12 (if we assume the loss per pass as equal to the transmittance).

It should be noted that the expression for the total power output, (47), is independent of the number of modes which oscillate. Different modes will in general (see Section XI) have different frequencies and different spatial characteristics so that for most applications only the power in a single mode can be utilized. If all the modes but one are suppressed the total power, corresponding to (47), will appear in this single mode. Kogelnik and Patel[65] were able to operate an He-Ne laser in a single fundamental mode. This was done by using frequency-sensitive reflectors. The power output was ~1.5 mw. A scheme for suppressing the transverse modes and limiting the oscillation to longitudinal modes has also been described by Burch[71] and by Skinner and Geusic.[72]

Having worked out detailed numerical examples for both the solid and gas lasers we are in a position to explain, at least partially, the relative ease of obtaining CW laser action in gases compared to solids. (Only four

[71] J. M. Burch, "Ruby masers with afocal resonators," *J. Opt. Soc. Am.*, vol. 52, p. 602; May, 1962.

[72] J. G. Skinner and J. E. Geusic, "Diffraction Limited Ruby Oscillator," Optical Society of America Program of the 47th Annual Meeting, Rochester, N. Y., p. 14, October, 1962.

solid CW lasers have been reported.) The comparison can be made by calculating the ratio of the number of transitions per second $\Delta N_c/t_{\text{spont}}$ (four-level operation is assumed) to the total number of atoms N_0. Using the following data:

$CaWO_4:Nd^{3+}$

$$\frac{\Delta N_c}{V} \sim 10^{16}, \qquad t_{\text{spont}} = 10^{-4} \text{ sec}, \qquad \frac{N_0}{V} \sim 10^{19}$$

He-Ne($\lambda \sim 1.15\,\mu$)

$$\frac{\Delta N_c}{V} \sim 10^{7}, \; t_{\text{spont}} = 10^{-7} \text{ sec}, \; \frac{N_0}{V} \sim 10^{16} \text{ (at 0.1 mm Hg)}$$

we get

$$CaWO_4:Nd^{3+} - \frac{\Delta N_c}{N_0 t_{\text{spont}}} \sim 10$$

$$\text{He-Ne} - \frac{\Delta N_c}{N_0 t_{\text{spont}}} \sim 10^{-2}.$$

The relative pumping rate in the gas laser is ~1000 times smaller than in the solid laser.

Optimum Coupling

A consideration of the conditions under which a given laser will yield maximum power output is of some importance. We shall follow Yariv[33] and define t_x and t_R by

$$\frac{1}{t_{\text{photon}}} = \frac{1}{t_R} + \frac{1}{t_x}. \tag{49}$$

$1/t_R$ is the contribution to the energy decay rate in the resonator due to all the loss mechanisms in the resonator (see Section IV) excluding the transmission loss. $1/t_x$ is the contribution due to the transmission, *i.e.*, due to the external coupling. The coupling ratio s is defined as

$$s = \frac{t_R}{t_x} \tag{50}$$

and is thus the ratio of the transmitted output power to that lost within the resonator. (It is also the ratio of the average mirror transmission per pass to the average loss per pass α.) The available power output is given by multiplying P in (47) by t_R/t_R+t_x. The result can then be used to solve for the optimum coupling condition. The result is

$$s_{\text{optimum}} = -1 + \sqrt{\text{PR}}. \tag{51}$$

The optimum coupling condition thus depends on the amount by which threshold is exceeded. For PR>4, the resonator should be overcoupled, *i.e.*, $s>1$. If sufficient pumping strength is available, say PR>4, the penalty in terms of reduced power output for using $s=1$ (critical coupling) instead of the exact value demanded by (51) is never larger than a factor of two. This is so because half the power is already available as output at $s=1$. The power result of ~1 watt quoted earlier in this section for a $CaF_2:U^{3+}$ laser was obtained with PR=5 and with dielectric mirrors of 3.5 per cent transmission which corresponded to $s \approx 1$.

Optimum coupling in a three-level laser obtains when

$$s = -1 + \sqrt{1 - \frac{N_0}{\Delta N_c}\frac{(1-\text{PR})}{(1+\text{PR})}}$$

where N_0 is the total number of atoms.

X. Noise in Lasers

Noise analyses for the microwave maser[73] show that the limiting effective input noise temperature[74,75] T_N for the case $h\nu \gg kT$ is

$$T_N = \frac{h\nu}{k \ln 2} \tag{52}$$

which is equivalent to stating that the effective input noise power in a bandwidth $d\nu$ in a maser amplifier is $\sim h\nu\, d\nu$. It has also been shown that this noise is due to spontaneous transitions.[76] The condition $h\nu \gg kT$ is amply fulfilled in the optical range. Taking as an example a laser operating at 1 μ at 290°K, the ratio $h\nu/kT$ is ~50, so that $T_N \sim 15{,}000$°K. This noise is referred to as quantum noise and it is necessary to avoid violation of the uncertainty principle in quantum mechanics.[73]

The spontaneous emission noise power is given by the critical fluorescence power

$$P_{fc} = \frac{ph\nu}{t_{\text{photon}}}. \tag{39}$$

This power is emitted into p modes (these should not be confused with the number of oscillating modes) so that the noise power per mode is $h\nu/t_{\text{photon}}$. The noise power in a single mode is distributed over the effective mode bandwidth $\Delta\nu \sim 1/t_{\text{photon}}$ so that the noise power in $d\nu \ll \Delta\nu'$ is $\sim h\nu\, d\nu$ which, as shown above, corresponds to $T_N \sim h\nu/k$.

A more rigorous treatment consists of recognizing that (39) corresponds to an equivalent excitation of the black body modes with $\bar{n}=1$. Using (9), where T be-

[73] R. Serber and C. H. Townes, "Limits on electromagnetic amplification due to complimentarity," *Proc. 1st Quantum Electronics Conf.*, Columbia University Press, New York, N. Y.; 1960.

[74] See, for instance, J. P. Gordon and L. D. White, "Noise in maser amplifiers—theory and experiment," Proc. IRE, vol. 46, pp. 1588–1594; September, 1958.

[75] T_N is related to the noise figure F by

$$F = 1 + \frac{T_N}{290}.$$

[76] R. V. Pound, "Spontaneous emission and the noise figure of maser amplifiers," *Ann. Phys.*, vol. 1, pp. 24–32; April, 1957.

A. Yariv and R. Kompfner, "Noise temperature in distributed amplifiers," IRE Trans. on Electron Devices, vol. ED-8, pp. 1–5; May, 1961.

comes T_N, yields

$$T_N = \frac{h\nu}{k \ln 2} \cdot \tag{53}$$

The spontaneous emission noise P_{fc} in three-level lasers was shown in Section V to be larger than in four-level lasers by a factor $N_2/\Delta N_c = \epsilon^{-1}$. The noise temperature for three-level lasers is thus given by $h\nu/\epsilon k \ln 2$. The increase in "noisiness" in the ruby laser, for example, is according to the numerical example of Section VI, ~50.

XI. Optical Resonators

We have already mentioned that the resonators used for laser oscillators usually take the form of a pair of opposing plane or curved reflectors, between which the radiation field propagates. The earliest realization of the importance of resonators of this type in generation of "microwave and infrared frequencies" seems to be that of Dicke.[77] Fig. 10 illustrates several mirror configurations, which are discussed in more detail below. In order for such a resonator to be able to support low loss, *i.e.*, long t_{photon}, or high Q field modes, it must satisfy two criteria. First, there must be a family of rays which, on suffering sequential specular reflections from the two reflectors, do not miss either reflector before making a reasonable number (say 20–100) of traversals. Second, the dimensions of the reflectors must satisfy the relation

$$\frac{a_1 a_2}{\lambda d} \gtrsim 1 \tag{54}$$

where a_1 and a_2 are half the widths of the two reflectors, respectively, in any arbitrary direction perpendicular to the resonator axis, and d is the distance between the reflectors. The first of these criteria, which follows from consideration of geometrical optics, is valid because the reflecting areas we are concerned with are large compared to a wavelength, and have radii of curvature which are also large compared to a wavelength. The second criterion follows from considerations of physical optics. One may think of it as requiring that the half angle subtended by one reflector at the second, say a_1/d, be somewhat greater than the half angle of the far field diffraction pattern of a nearly plane wave originating at and restricted to the dimension of the second, *i.e.*, $\lambda/2a_2$.

Theoretical studies of the modes of such resonators have been made by Fox and Li,[78] Boyd and Gordon,[79] and Boyd and Kogelnik,[80] and most of their predictions have been verified experimentally by Kogelnik and Rigrod.[81] The transmission line duals of these resonators, in which the two reflectors are replaced by a periodic sequence of lenses, have been studied independently by Goubau and Schwering.[82]

There are, of course, many structures which exhibit electromagnetic resonances at optical frequencies. Since, however, the density of modes at optical frequencies is so large, the problem of creating a structure which has only a few high Q resonances within the line width of the amplifying transition is not trivial. For example, laser oscillations have been produced in the total internal reflection modes of dielectric spheres by Garrett, *et al.*,[83] but single modes have not been observed in this structure. Laser action in single transverse modes of glass fibers a few wavelengths in diameter, which act as dielectric waveguides, has been demonstrated by Snitzer.[84] In this case the volume of active material and thus the available power is necessarily quite small.

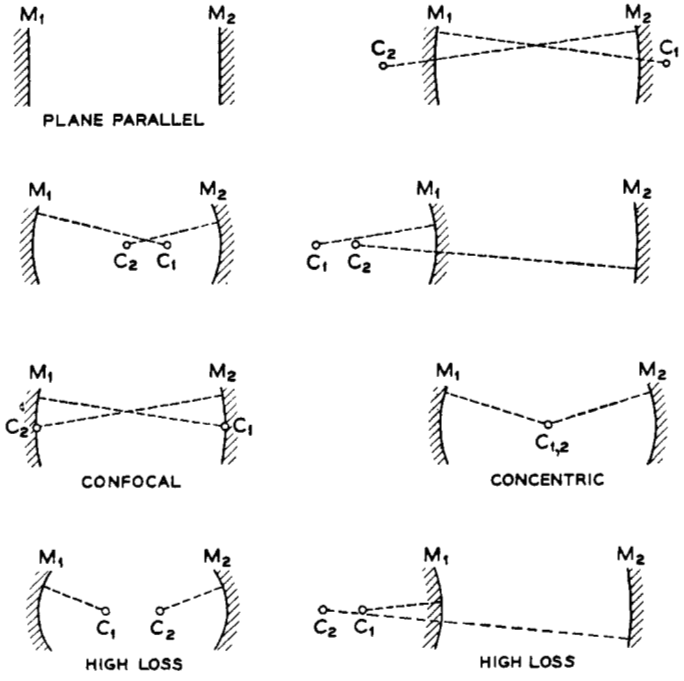

Fig. 10—Examples of mirror configurations for optical masers. All except the bottom two exhibit low-loss resonant modes.

[77] R. H. Dicke, "Molecular Amplification and Generation Systems and Methods," U. S. Patent No. 2,851,652; September 9, 1958.

[78] A. G. Fox and T. Li, "Resonant modes in a maser interferometer," *Bell Sys. Tech. J.*, vol. 40, pp. 453–458; March, 1961.

[79] G. D. Boyd and J. P. Gordon, "Confocal multimode resonator for millimeter through optical wavelength masers," *Bell Sys. Tech. J.*, vol. 40, pp. 489–508; March, 1961.

[80] G. D. Boyd and H. Kogelnik, "Generalized confocal resonator theory," *Bell Sys. Tech. J.*, vol. 41, pp. 1347–1371; July, 1962.

[81] H. Kogelnik and W. W. Rigrod, "Visual display of isolated optical resonator modes," Proc. IRE (*Correspondence*), vol. 50, p. 220; February, 1962.

[82] G. Goubau and F. Schwering, "On the guided propagation of electromagnetic wave beams," IRE Trans. on Antennas and Propagation, vol. AP-9, pp. 248–255; May, 1961.

[83] C. G. B. Garrett, W. Kaiser, and W. L. Bond, "Stimulated emission into optical whispering modes of spheres," *Phys. Rev.*, vol. 124, pp. 1807–1809; December, 1961.

[84] E. Snitzer, "Cylindrical dielectric waveguide modes," *J. Opt. Soc. Am.*, vol. 51, pp. 491–498; May, 1961.

E. Snitzer and H. Osterberg, "Observed dielectric waveguide modes in the visible spectrum," *J. Opt. Soc. Am.*, vol. 51, pp. 499–505; May, 1961.

We will restrict the detailed discussion to the open two-mirror structure, for which the vast majority of modes have high losses. The remaining high Q modes then take the form of almost plane wave beams which propagate back and forth between the reflectors.

By analogy to waveguide theory, we can discuss these modes in terms of a set of field configurations over the surfaces of the reflectors. Such a field configuration is called a transverse mode, if, after propagation from one reflector to the other and back, the field returns in the *same* pattern, multiplied by a complex number which gives the total phase shift and loss of the round trip. For every such transverse mode, there is then a sequence of longitudinal modes, for which the round trip phase shift is an integral multiple of 2π. Since the waves are nearly plane waves, the spacing of longitudinal modes for a given transverse mode is just

$$\Delta\nu = c/2d$$

where d is the distance between reflectors, and c is the velocity of light in the resonator medium. If the medium gain makes up for the total round trip loss (including transmission loss) then laser oscillation will occur.

The problem of finding the transverse modes has been attacked in two ways. One is to seek simple solutions to Maxwell's equations which take the form of narrow beams, and then to make the reflection surfaces intersect the beam along phase fronts, *i.e.*, everywhere perpendicular to the local direction of propagation, thus insuring the reflection of the wave back exactly on itself. The other method, introduced by Fox and Li,[78] is to use the scalar formulation of Huygens' principle to compute the field at one mirror caused by the illumination of the other. The return field configuration is similarly calculated and is then required to match, within a constant, the initial field configuration. Solutions of the resulting integral equation yield the modes and the diffraction losses. This method is adaptable to numerical machine calculations for situations where analytical methods are not available. These two methods yield qualitatively similar results.

Let us consider the simple beam solutions to Maxwell's equations. These are characterized by a direction of propagation, which we take as the z axis, and by a plane phase front perpendicular to this axis which we take as the plane $z=0$. In this plane the electric field is everywhere parallel to a given direction in the plane, which we can take as the x axis. In the plane the field amplitude of the m, n mode has the form[79]

$$E_{m,n}^{(x)} = E_0 H_m\left(\sqrt{2}\,\frac{x}{\omega_0}\right) H_n\left(\sqrt{2}\,\frac{y}{\omega_0}\right) \exp\left(-\frac{x^2+y^2}{\omega_0^2}\right)$$

where H_m and H_n are Hermite polynomials of order m and n respectively, and ω_0 is a parameter with dimensions of length, which must be somewhat larger than λ for the theory to hold. We note that the modes with different m or n are orthogonal to each other over the plane. Photographed field patterns, originally obtained by Kogelnik and Rigrod,[80] are shown in Fig. 11.

Such a wave, traveling toward $+z$, has $H_y = E_x$ (in Gaussian units). As it propagates it maintains its form, but spreads by diffraction. The local directions of propagation follow hyperbolic curves, as in Fig. 12. Over the spherical surfaces of constant phase orthogonal to these hyperbolae[85] the field amplitude has the form[79,86]

$$E_{m,n}^{(x)} = E_0 \frac{w_0}{w} H_m\left(\sqrt{2}\,\frac{x}{w}\right) H_n\left(\sqrt{2}\,\frac{y}{w}\right) \cdot \exp\left(-\frac{x^2+y^2}{w^2}\right) \tag{55}$$

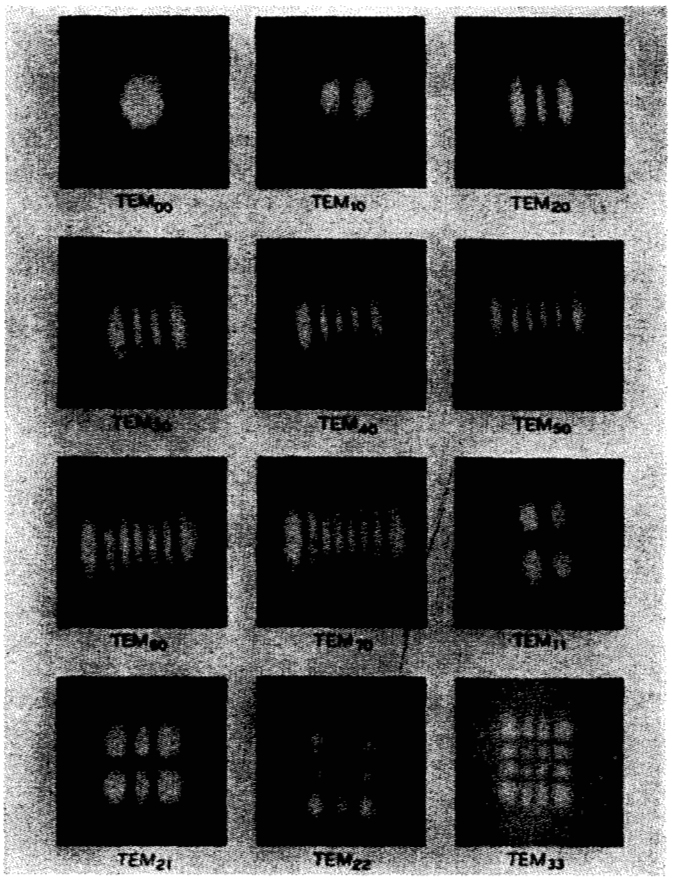

Fig. 11—Some low-order single-mode field patterns.

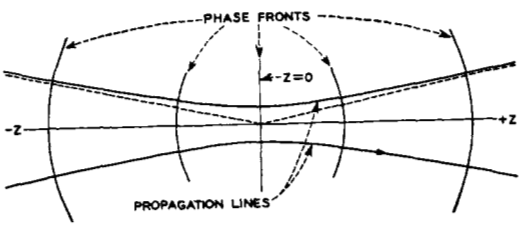

Fig. 12—Hyperbolic curves corresponding to the local directions of propagation.

[85] Actually, these surfaces are not quite spherical, but for the important region near the z axis they may be considered spherical.

[86] We have labeled the field as though it were x directed. Actually it is tangent to the constant phase surfaces.

where

$$w = w_0\left[1 + \left(\frac{z}{z_0}\right)^2\right]^{1/2}; \qquad z_0 = \frac{\pi w_0^2}{\lambda}$$

and λ is the wavelength of a plane wave in the resonator medium. The hyperbolae are intersections of planes which include the z axis and the hyperboloids

$$x^2 + y^2 = \text{const} \times w^2$$

while the spherical surfaces which represent possible positions of reflectors have radii of curvature R given by

$$R(z) = -w\frac{dz}{dw} = -\frac{1}{z}[z^2 + z_0^2]. \tag{56}$$

These beam modes give quite accurately the transverse modes of a resonator provided the two reflectors lie along phase fronts *and* are large enough to intercept substantially all of the field. The hyperboloid $x^2+y^2=w^2$ is the locus of points where the exponential factor in the field amplitude falls to exp (-1). The distance w has therefore been defined as the "spot size" of the dominant $(m=n=0)$ mode. For large z this hyperboloid is asymptotic to the cone

$$x^2 + y^2 = \left(\frac{\lambda}{\pi w_0}\right)^2 z^2 \tag{57}$$

whose half apex angle is $\tan^{-1}(\lambda/\pi w_0)$. This we recognize as the diffraction angle of a nearly plane wave limited to an area of dimension $\approx \pi w_0$, and the restriction $w_0 > \lambda$ means the solutions are valid only for beams for which this apex angle is reasonably small.

To complete the picture we need the propagation constant. Along the z axis the phase variation is given by

$$kz - (m + n + 1)\tan^{-1}\left(\frac{z}{z_0}\right) \tag{58}$$

which is a convenient re-expression of a result of Boyd and Gordon.[79] We note here an essential degeneracy of all modes with the same $m+n$, since they all have the same phase variation with z. Thus any linear combination of modes with the same value of $m+n$ will also be a mode and will propagate without any change in form. One such set of linear combinations gives modes whose analytic form is separated in cylindrical coordinates. In this form which appears in the work of Goubau and Schwering,[82] the modes are

$$E_{p,l}^{(z)} = E_0'\left(\frac{w_0}{w}\right)\left(\frac{r}{w}\right)^l\left(\begin{Bmatrix}\sin\\ \cos\end{Bmatrix} l\theta\right) L_p^l\left(2\frac{r^2}{w^2}\right) \cdot \exp\left(-\frac{r^2}{w^2}\right)$$

where the L_p^l are the associated Laguerre polynomials, and the phase along z is given by

$$kz - (2p + l + 1)\tan^{-1}\left(\frac{z}{z_0}\right).$$

Given these beam modes, we see how to make a resonator. We simply insert two reflectors which match two of the spherical surfaces defined by (56). Alternatively, given two mirrors with spherical curvature and some distance of separation, if the position of the plane $z=0$ and the value of the parameter w_0 can be adjusted so that the mirrors coincide with two such surfaces, we will have found the modes. If, in addition, the mirrors are large enough to intercept, say, 99 per cent of the energy of the $m=n=0$ mode then that mode will have about a 1 per cent loss by diffraction in each reflection. The modes with large m and n have fields extending farther out from the axis and so will suffer larger diffraction losses. In this way one can discriminate between the transverse modes, and ensure that only a few will have low loss. It turns out that the mirror configurations for which the matching of surfaces is possible are just those which satisfy the first stability criterion mentioned at the beginning of this section which was based on ray optics. A fairly simple rule for finding the allowed values of mirror curvatures and separation is as follows. Consider the two mirrors, their centers of curvature, and the axis of the resonator, which is the line joining the two centers. The rule states that either the center of curvature of one mirror or that mirror itself, but not both, must cut the axis between the other mirror and its center of curvature. This rule is obviously reciprocal; it does not matter which mirror one starts with. Some examples of mirror configurations are shown in Fig. 10.

To gain an understanding of how the modes vary with the parameters, consider the rather simple situation which occurs when one mirror is plane. The plane $z=0$ must then be coincident with this mirror. Let the other mirror be placed at $z=d$ (d is then the distance separating the mirrors) and have radius of curvature $-R$, where the minus sign indicates that the center of curvature lies to the $-z$ side of the mirror. Then, using (56) and (55), with $R(z)=-R$, we see that

$$z_0 = (Rd - d^2)^{1/2}$$

$$w_0 = \left(\frac{\lambda z_0}{\pi}\right)^{1/2} = \left(\frac{\lambda d}{\pi}\right)^{1/2}\left(\frac{R-d}{d}\right)^{1/4} \tag{59}$$

and

$$w = \left(\frac{\lambda d}{\pi}\right)^{1/2}\left[\frac{R^2}{d(R-d)}\right]^{1/4}$$

where w is the spot size on the curved reflector, while w_0 is the spot size on the plane reflector. Note that for

$R \gg d$, both spot sizes are very nearly the same and are given by

$$w(R \gg d) = \left(\frac{\lambda d}{\pi}\right)^{1/2}\left(\frac{R}{d}\right)^{1/4}. \tag{60}$$

For this case the wave propagates between reflectors without spreading appreciably; *i.e.*, as a plane wave. As R approaches d, w_0 decreases and w increases without limit, but of course the theory becomes invalid as $w_0 \to \lambda$. For $R < d$ the theory gives unphysical answers (*i.e.*, imaginary spot sizes), and in fact this is in the region where low-loss modes do not exist by the ray criterion. Thus we must have $R \geq d$. The product of the spot sizes is given by

$$ww_0 = \frac{\lambda}{\pi}(Rd)^{1/2}.$$

Since the mirrors must be somewhat larger than the spot sizes for these solutions to represent the modes, and $R \geq d$, we see that the original second criterion [see (54)] for the existence of low-loss modes is satisfied.

If we let R approach ∞ or d we can satisfy the second criterion with mirrors which are substantially smaller than the spot size. For such cases low-loss modes do exist, but machine computations are necessary to obtain their patterns. The extreme cases $R = d$, $R = \infty$ have been computed by Fox and Li,[78] who also considered such perturbations as mirror tilt, etc.

Fig. 13 shows the computed losses for the plane parallel resonator and for the symmetrical confocal resonator which has the minimum spot size for a given separation, and thus the minimum loss. Other allowed curvatures give intermediate losses. To give a numerical example, let us take the following numbers typical of a gas laser:

$$\lambda = 10^{-4} \text{ cm (1 micron)}$$
$$d = 10^{2} \text{ cm}$$

and suppose that in front of the curved mirror is an aperture of radius

$$a = 0.3 \text{ cm}.$$

We have

$$\left(\frac{\lambda d}{\pi}\right)^{1/2} = 0.06 \text{ cm}.$$

The minimum spot size w occurs [see (59)] for $R = 2d$, where

$$w_{\min} = \left(\frac{2\lambda d}{\pi}\right)^{1/2} = 0.080 \text{ cm}.$$

In order that the spot size equal the aperture radius a, we require from (56) that

$$\left(\frac{R}{d}\right) = \left(\frac{0.3}{0.06}\right)^{4} \sim 600$$

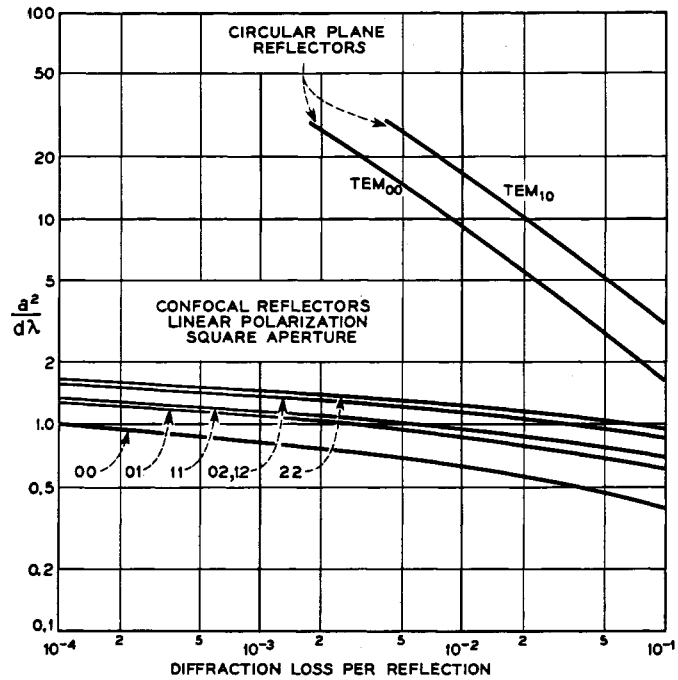

Fig. 13—Diffraction losses for plane-parallel and confocal resonators.

whence $R = 600$ meters. Thus to attain spot size only four times the minimum, the mirrors must both be exceedingly plane. This result has immediate consequences for the solid-state lasers, where inhomogeneities in the optical quality of the medium give rise to local variations in the optical path, with the resultant "filaments" of oscillation occurring at local maxima in the path length.

XII. Some Characteristics of Lasers

The many potential applications of lasers, some of which are discussed in Section XIII, stem mostly from the laser's high degree of temporal and spatial coherence. Since these two terms are often used vaguely it is probably worthwhile to be more precise.

The temporal coherence for the field oscillation at a point r is specified by the correlation function $\pi(\tau)$

$$\pi(\tau) = \overline{\boldsymbol{E}(r,t)\cdot\boldsymbol{E}(r,t+\tau)} \tag{61}$$

which is the time average (indicated by the bar) of the scalar product of two values of the field at the same point in space but separated in time by τ. For a plane-polarized wave of a narrow spectral bandwidth centered around an angular frequency ω_0, $\pi(\tau)$ has the form

$$f(\tau)\cos(\omega_0\tau) \tag{62}$$

and the "coherence time" of the wave τ_c is defined as the value of τ for which $f(\tau)/f(0)$ falls to some fixed, say $1/e$, value. Since the spectral power density function (the square of the Fourier transform) of $E(t)$ is given by the Fourier transform of $\pi(\tau)$ it follows that the spectral bandwidth of the field oscillation $\Delta\nu_s$ is $\sim 1/\tau_c$.

The finite coherence time of the laser is a consequence of the equivalent noise power $h\nu d\nu$ which, as shown in Section X, is due to spontaneous emission.

The total width at half-power $\Delta\nu_s$ of the spectral distribution function for an oscillator with an equivalent noise energy $h\nu$ in the resonator mode is given as[87]

$$\Delta\nu_s \sim \frac{8\pi h\nu(\Delta\nu')^2}{P} \tag{63}$$

where

$$\Delta\nu' \sim \frac{1}{t_{\text{photon}}} .$$

Using the following data for a typical He-Ne laser

$$\nu \sim 3 \times 10^{14} \text{ cps}$$
$$L = 1 \text{ m}$$
$$\alpha(\text{loss per pass}) = 2 \text{ per cent}$$
$$P = 1 \text{ mw}$$
$$\Delta\nu' \sim 6 \times 10^{6} \text{ cps}$$

yields

$$\Delta\nu_s \sim 4 \times 10^{-1} \text{ cps.}$$

Short-time frequency stabilities of ~50 cps have been reported.[88]

Spatial coherence is specified by correlation functions of the form

$$\overline{E_x(r, t)E_x(r + \Delta r, t)} \tag{64}$$

which is the time average of the product of two field components taken at the same time but at different positions in space. For narrow beams of radiation one usually restricts the idea of spatial coherence to vectors Δr which are perpendicular to the direction of propagation of the beam, since "spatial" coherence along the direction of propagation is intimately related to temporal coherence.

A beam in the form of a single transverse mode is, by the definition of a mode, spatially coherent over the whole cross section of the beam; thus it is possible to do optical operations on such a beam limited only by diffraction. In particular the TEM_{00} mode can be focused by a diffraction-limited lens to a spot of radius [see (57)];

$$w_0 = \frac{\lambda}{\pi\alpha}$$

where α is the tangent of the half apex angle of the cone of converging light. [$(2\alpha)^{-1}$ is then the f-number of this cone.] If the beam contains the lowest N transverse modes the area of the spot simply increases in proportion to N. The power density and field strength in such a spot can be very high. Thus, ten joules from a ruby laser, fired in 10 nsec, focused to a spot 0.1 mm in diameter (f-number − 10, $N = 100$) gives a power density of about 10^{13} watts/cm^2, and a field strength of nearly 10^8 volts/cm.

A striking demonstration of the large degree of spatial coherence of the ruby laser was the two slit interference pattern obtained by Nelson and Collins[89] in an experiment in which the light output of the laser was used to illuminate the slits directly.

XIII. Applications

The great number of applications envisaged for lasers is still a matter of the future. These applications await the solution of numerous secondary problems such as: increased power output, satisfactory means for wide bandwidth modulation and detection, long time frequency stability, single mode operation, new wavelengths, and others. Some of these applications are:

1) *Medicine*—Laser beams focused to a small spot size have been used to repair detached retinas and for localized removal of malignant tissue.[90]
2) *Industrial*—Some demonstrations in which laser beams have been used for drilling of small (~1/1000-inch) holes in diamond, steel, and other hard materials have been described.[90] These are probably only the forerunners of numerous other applications.
3) *Photography*—The availability of intense laser light pulses has been used to increase the time resolution of high-speed photography.[91]
4) *Scientific Applications*—The behavior of atoms and ions under the influence of intense and coherent fields at optical frequencies is largely an unexplored field. Porto and Wood have demonstrated the use of the laser in Raman spectroscopy.[92]
5) *Bridging the Spectrum Gap*—No coherent oscillators are now available between $\lambda \sim 500\,\mu$ (0.5 mm) and $\lambda \sim 13\,\mu$. It is unlikely that conventional microwave sources such as backward-wave oscillators, klystrons, and magnetrons will bridge this gap. There is, however, no fundamental reason why lasers cannot be made to operate over this frequency range. Numerous problems in physics, specifically in superconductivity, spectroscopy, and antiferromagnetism, to mention a few, are already clamoring for signal sources in this range.

[87] J. P. Gordon, H. J. Zeiger, and C. H. Townes, "The maser—new type of microwave amplifier, frequency standard, and spectrometer," *Phys. Rev.*, vol. 99, pp. 1264–1274; August 15, 1955.
[88] A. Javan, private communication.
[89] D. F. Nelson and R. J. Collins, "Spatial coherence in the output of an optical maser," *J. Appl. Phys.*, vol. 32, pp. 739–740; April, 1961.
[90] M. Hurwitz, "Lasers—will their potential be realized," *Solid State Design*, vol. 3, pp. 68–71; September, 1962.
[91] J. S. Courtney-Pratt, "Some uses of optical masers in photography," *J. SMPTE*, vol. 70, pp. 509–511; July, 1961.
[92] S. P. S. Porto and D. L. Wood, "Ruby optical maser as a Raman source," *J. SMPTE*, vol. 52, pp. 251–252; March, 1962.

6) *Parametric Optics*—The extension of parametric and harmonic generation techniques to optical frequencies has already been demonstrated by experiments by Franken, *et al.*,[93] Bass, *et al.*,[94] Giordmaine,[95] and Maker, *et al.*[96] The two-photon excitation experiment of Kaiser and Garrett[97] is also of interest in this connection. Eckhardt, *et al.*,[98] reported the operation of a pulsed organic Raman laser which was pumped by the output from a pulsed ruby laser. The operation of this device can be described, very roughly, as a parametric interaction between the pumping laser light and the natural frequencies of vibration of the liquid molecules which combine to yield a coherent oscillation at the difference frequency. The theory of the Raman laser has been worked out by Hellwarth.[99]
7) *Standards*—Lasers may provide excellent frequency and length standards because of their long coherence time. Although laser frequencies cannot as yet be measured directly, two laser frequencies which differ by a directly measurable frequency (microwave or lower) can be very accurately compared. Since the laser frequency is very sensitive to the mirror separation, its application as a strain gauge or seismograph is suggested.[100]

An intensification of the peak power from pulsed solid lasers by "Q switching" has been proposed by Hellwarth[101] and demonstrated by McClung and Hellwarth.[102] A Kerr-cell switch was used to degrade the resonators Q for the duration of the pumping pulse. This made it possible to achieve a larger population inversion without oscillation. Restoration of the Q to its original value resulted in an output pulse with peak intensity several orders of magnitudes larger than in normal operation. The practical importance of this scheme can be appreciated when one realizes that most of the industrial applications proposed to date rely on short and intense pulses.

[93] P. A. Franken, A. E. Hill, C. W. Peters, and G. Weinreich, "Generation of optical harmonics," *Phys. Rev. Lett.*, vol. 7, pp. 118–119; August, 1961.
[94] M. Bass, P. A. Franken, A. E. Hill, C. W. Peters, and G. Weinreich, "Optical mixing," *Phys. Rev. Lett.*, vol. 8, pp. 18; January, 1962.
[95] J. A. Giordmaine, "Mixing of light beams in crystals," *Phys. Rev. Lett.*, vol. 8, pp. 19–20; January, 1962.
[96] P. D. Maker, R. W. Terhune, M. Nisenoff, and C. M. Savage, "Effects of dispersion and focusing on the production of optical harmonics," *Phys. Rev. Lett.*, vol. 8, pp. 21–22; January, 1962.
[97] W. Kaiser and C. G. B. Garrett, "Two-photon excitation in CaF_2:Eu^{2+}," *Phys. Rev. Lett.*, vol. 7, pp. 229–231; September, 1961.
[98] G. Eckhardt, R. W. Hellwarth, F. J. McClung, S. E. Schwarz, D. Weiner, and E. J. Woodbury, "Stimulated Raman Scattering from Organic Liquids," to be published.
[99] R. W. Hellwarth, "The Theory of Stimulated Raman Scattering from Organic Liquids," to be published.
[100] A. Javan, private communication.
[101] R. W. Hellwarth, "Control of fluorescent pulsations," in "Advances in Quantum Electronics," J. R. Singer, Ed., Columbia University Press, New York, N. Y., pp. 334–342; 1961.
[102] R. W. Hellwarth and F. J. McClung, "Giant optical pulsations from ruby," *Bull. Am. Phys. Soc.*, vol. 6, p. 414; November, 1961.

XIV. Lasers in Communications

As shown in Section XI we may consider the dominant resonator mode as a finite plane wave which, because of diffraction, propagates as a conical beam with half apex angle given by [see (53)]

$$\alpha = \tan^{-1}\left(\frac{\lambda}{\pi w_0}\right) \approx \frac{\lambda}{\pi w_0}.$$

The spot size of the dominant mode w_0 can be increased by the use of mirrors or lenses to any size, which is limited only by the accuracy with which these optical components can be made (*i.e.*, the optics must remain diffraction-limited). If w_0 is made, say 15 cm, the initial wavefront is plane and λ is 10^{-4} cm, then

$$\alpha = 2 \times 10^{-6} \text{ radians} \cong \text{sec of arc}.$$

Such precise angular resolution, attainable with "antennas" of quite small physical dimensions, suggests that the laser may be useful for communications,[103,104] for radar,[105] and perhaps in some special cases for power transmission, although the rather low over-all efficiency of the present lasers would seem to militate against the power transmission idea.

In communications, of which radar is a special example, the laser may find important usefulness. The information capacity of a communications channel depends on the bandwidth of the channel and on the signal-to-noise ratio achieved at the receiver. As discussed in Section X, ordinary thermal noise is negligibly small at optical frequencies; instead, quantum noise plays the basic role in limiting the capacity.[104] Thus, even though a signal in a single transverse mode from a CW oscillator is observed, an energy detector will respond with a random sequence of photoelectron emissions, *i.e.*, it will exhibit shot noise; a laser amplifier will degrade the signal by the addition of its spontaneous emission noise, while a heterodyne or homodyne converter[106] adds noise by virtue of the shot noise in the photocurrent generated by the local oscillator.

Consider first the case of an energy-sensitive receiver (for example, a simple photocell). Suppose the quantum efficiency of the photosurface is ϵ, and a pulse whose expected energy is E_0 strikes it. The probability $p(n)$ that n photoelectrons are ejected from the surface is then given by the Poisson distribution

$$p(n) = \frac{1}{n!}\left(\frac{\epsilon E_0}{h\nu}\right)^n \exp\left(-\frac{\epsilon E_0}{h\nu}\right)$$

[103] D. G. C. Luck, "Some factors affecting applicability of optical-band radio (coherent light) to communication," *RCA Rev.*, vol. 22, pp. 359–409; September, 1961.
[104] J. P. Gordon, "Quantum effects in communications systems," Proc. IRE, vol. 50, pp. 1898–1908; September, 1962.
[105] D. A. Budenhagen, *et al.*, "An experimental laser ranging system," 1961 IRE International Convention Record, pt. 5, pp. 185–193.
[106] B. M. Oliver, "Comments on 'Noise in photoelectric mixing'," Proc. IRE (*Correspondence*), vol. 50, pp. 1545–1546; June, 1962.

for which the average, or expected, number of photoelectrons is

$$\langle n \rangle = \frac{\epsilon E_0}{h\nu}.$$

To be quite sure of detecting the pulse, we might require that

$$p(0) = \exp\left(-\frac{\epsilon E_0}{h\nu}\right) < 10^{-6}$$

whence

$$E_0 > \frac{14}{\epsilon} h\nu.$$

Thus, each received pulse must contain about $14/\epsilon$ photons if it is to be reliably detected, and then the information rate depends simply on the pulse repetition rate. If this repetition rate is B,[107] and the pulses are sent with 50 per cent probability so that each interval B^{-1} carries one bit of information, then the information rate R is equal to the repetition rate. Thus

$$R = B$$

for a received power

$$P = \frac{1}{2} E_0 B > \frac{7}{\epsilon} h\nu B.$$

The role of the laser in such a system would be as a transmitter, to ensure the greatest possible received power. Its temporal coherence would not be utilized in an important way. The dark current of the photodetector, and its response to the ambient illumination within its field of view are other important sources of noise in such a system, and would tend to increase the required signal power.

Consider now the use of a laser as an amplifier of an optical signal, which is presumed to exist in a single transverse mode. Assuming that the amplifier has high gain, the spontaneous emission noise which enters the signal mode has an equivalent input power of

$$\frac{1}{\epsilon} h\nu B$$

where $\epsilon = 1 - N_1/N_2$, N_1 and N_2 being the lower- and upper-state populations in the laser medium, and where B is the amplifier bandwidth. We have used the same symbol ϵ here as for the quantum efficiency of the detector since the roles played by the two ϵ's are very similar.

[107] We use the symbol B since the minimum bandwidth consistent with this repetition rate is B.

Thus, an output SNR greater than unity requires a received signal power

$$P > \frac{1}{\epsilon} h\nu B.$$

The spontaneous emission noise is additive and Gaussian;[108] its effects (presuming high gain) can thus be completely understood from classical noise theory. To obtain reliable communication at an information rate comparable to the bandwidth, one might require an SNR of, say, 20 db, whence

$$P \sim \frac{100}{\epsilon} h\nu B;$$

as in the case of energy detection, one needs a received signal somewhat in excess of $h\nu B$. In this case the detector following the amplifier must be made sensitive only to the signal mode to avoid excessive noise.

At a wavelength of one micron ($\nu = 3 \times 10^{14}$ c/sec),

$$h\nu = 2 \times 10^{-19} \text{ joules.}$$

This may be compared to the standard kT_0 ($T_0 = 290°$) of

$$kT_0 = 4 \times 10^{-21} \text{ joules.}$$

Thus, any optical system is reasonably noisy by microwave standards; *i.e.*, $50/\epsilon$ times as noisy as a 3-db noise figure microwave system. Nonetheless, its peculiar advantages of small antenna size and the possibility of low-loss transmission[82] should make such systems quite useful.

A number of topics which are closely related to laser theory but do not involve it directly have been omitted. Among these are the experiments of Forrester[109] and of McMurtry and Siegman[110] and of Riesz[111] on photoelectric detection and of Kaminow[112] on high-speed modulation of light.

Acknowledgment

The paper benefited generously from critical reading and numerous suggestions by G. D. Boyd, C. C. Cutler, W. L. Faust, C. G. B. Garrett, D. F. Nelson and S. P. S. Porto.

[108] J. P. Gordon, W. H. Louisell, and L. R. Walker, "Quantum statistics of maser amplifiers and attenuators," to be published.

[109] A. T. Forrester, "Photoelectric mixing as a spectroscopic tool," *J. Opt. Soc. Am.*, vol. 51, pp. 253–259; March, 1961.

[110] B. J. McMurtry and A. E. Siegman, "Photomixing experiments with a ruby optical maser and a traveling wave tube," *Appl. Optics*, vol. 1, pp. 51–53; January, 1962.

[111] R. P. Riesz, "High speed semiconducting photodiode," *Rev. Sci. Instr.*, vol. 33, pp. 994–998; September, 1962.

[112] I. P. Kaminow, "Microwave modulation of the electro-optic effect in KH_2PO_4," *Phys. Rev. Lett.*, vol. 6, pp. 528–530; May, 1961.

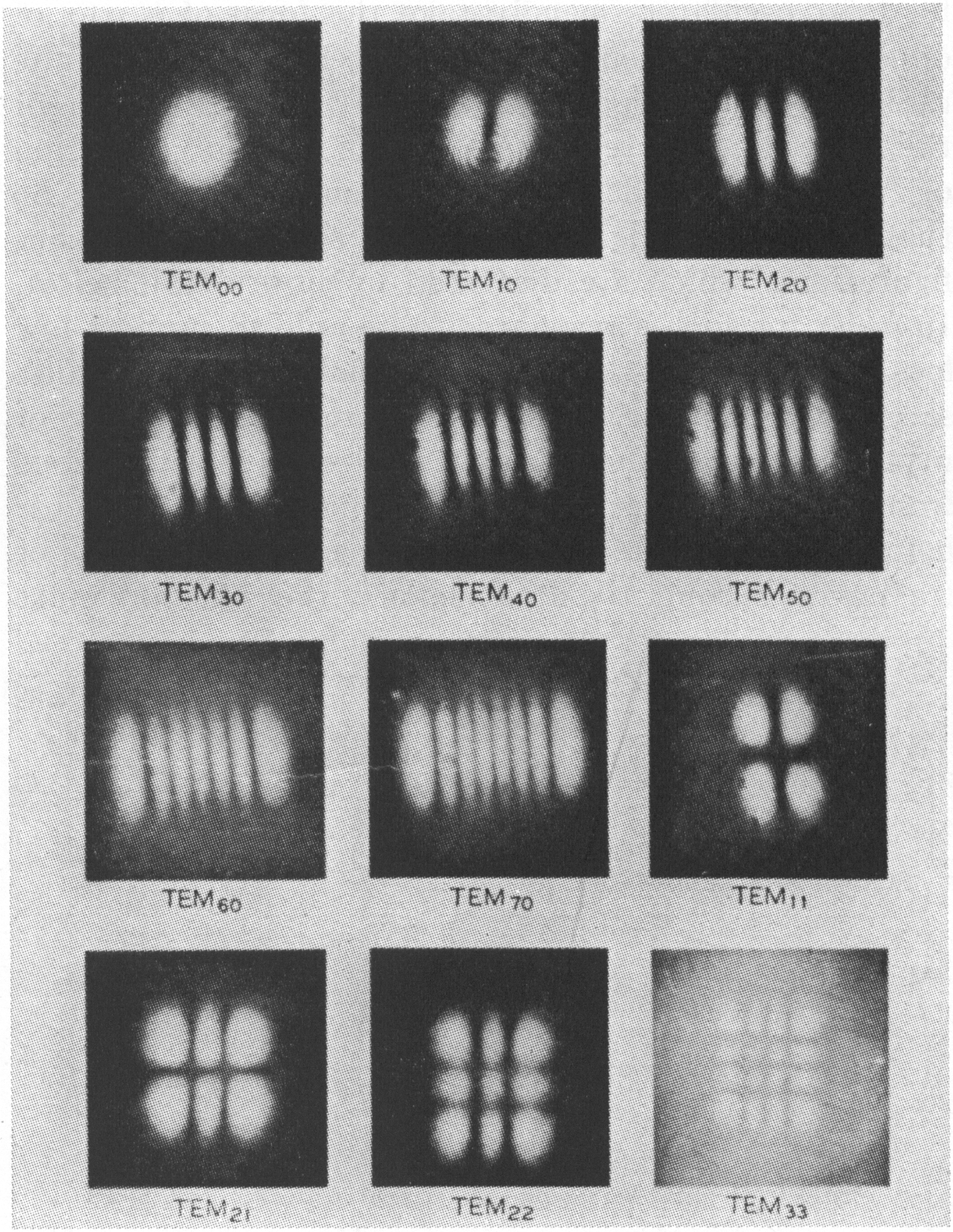

Fig. 11—Some low-order single-mode field patterns.